HHS Public Access

Author manuscript

FASEB J. Author manuscript; available in PMC 2021 February 01.

Published in final edited form as:

FASEB J. 2020 February ; 34(2): 2126–2146. doi:10.1096/fj.201901301R.

Increased expression of desmin and vimentin reduces bladder smooth muscle contractility via JNK2

Elham Javed[1], **Chellappagounder Thangavel**[2], **Nagat Frara**[3], **Jagmohan Singh**[4], **Ipsita Mohanty**[4], **Joseph Hypolite**[1], **Ruth Birbe**[5], **Alan S. Braverman**[3], **Robert B Den**[2], **Satish Rattan**[4], **Stephen A Zderic**[6], **Deepak A Deshpande**[1], **Raymond B. Penn**[1], **Michael R. Ruggieri Sr**[3], **Samuel Chacko**[7,8], **Ettickan Boopathi**[1,7]

[1]Department of Medicine, Center for Translational Medicine, Thomas Jefferson University, Philadelphia, Pennsylvania

[2]Department of Radiation Oncology, Thomas Jefferson University, Philadelphia, Pennsylvania.

[3]Department of Anatomy and Cell Biology, Lewis Katz School of Medicine, Temple University, Philadelphia, Pennsylvania.

[4]Department of Medicine, Division of Gastroenterology & Hepatology, Thomas Jefferson University, Philadelphia, Pennsylvania.

[5]Department of Pathology and Laboratory Medicine, Cooper University Health Care, Camden, NJ.

[6]Department of Urology, Children's Hospital of Philadelphia, Philadelphia, Pennsylvania

[7]Division of Urology, University of Pennsylvania, Philadelphia, Pennsylvania.

[8]Department of Pathobiology, University of Pennsylvania, Philadelphia, Pennsylvania.

Abstract

Bladder dysfunction is associated with overexpression of the intermediate filament (IF) proteins desmin and vimentin in obstructed bladder smooth muscle (BSM). However, the mechanisms by which these proteins contribute to BSM dysfunction are not known. Previous studies have shown that desmin and vimentin directly participate in signal transduction. In this study, we hypothesized that BSM dysfunction associated with overexpression of desmin or vimentin is mediated via c-Jun N-terminal kinase (JNK). We employed a model of murine BSM tissue in which increased expression of desmin or vimentin was induced by adenoviral transduction to examine the sufficiency of increased IF protein expression to reduce BSM contraction. Murine BSM strips overexpressing desmin or vimentin generated less force in response to KCl and carbachol relative to the levels in control murine BSM strips, an effect associated with increased JNK2 phosphorylation and reduced myosin light chain (MLC_{20}) phosphorylation. Furthermore, desmin

Corresponding Author: Boopathi Ettickan, PhD, Assistant Professor, Center for Translational Medicine, Thomas Jefferson University, Philadelphia, Pennsylvania. boopathi.ettickan@jefferson.edu.

Author Contributions

E. Javed and E. Boopathi designed the studies, performed the experiments, analyzed and interpreted the data and wrote the manuscript. DA Deshpande, RB. Penn and MR. Ruggieri Sr. contributed to design of studies, data analysis, writing of the manuscript. C. Thangavel, N. Frara, J. Singh, I. Mohanty, J. Hypolite and R. Birbe performed the experiments and analyzed the data. AS. Braverman, S. Rattan, RB. Den, SA Zderic, and S. Chacko analyzed data and contributed to the writing of the manuscript

The authors declare that they have no conflict of interest with the contents of this article.

and vimentin overexpression did not alter BSM contractility and MLC_{20} phosphorylation in strips isolated from JNK2 knockout mice. Pharmacological JNK2 inhibition produced results qualitatively similar to those caused by JNK2 knockout. These findings suggest that inhibition of JNK2 may improve diminished BSM contractility associated with obstructive bladder disease.

Keywords

Intermediate filaments; KCl; carbachol; cholinergic agonist; bladder

Introduction

Intermediate (10 nm) filaments (IFs) are involved in maintaining intracellular integrity, cell morphology integrating mechanical properties of the contractile apparatus, mechanochemical signaling, force transmission, and in regulating sub-cellular organelle structure and function (1, 2), (3–6). In smooth muscle, these IFs have been proposed to be coupled to the contractile units through dense bodies (7). IFs in smooth muscle form homopolymers or heteropolymers of desmin and vimentin filaments which constitute one of the major components of the cytoskeleton (6, 8, 9). Based on their structural and sequence homology, desmin and vimentin proteins are classified under type III IFs (6, 8). Desmin is a muscle- specific protein expressed in skeletal, cardiac and smooth muscle (1, 2). In normal (healthy) visceral smooth muscle such as bladder, desmin is the sole component of IF, whereas vimentin is not expressed (2). However, studies of animal models of partial bladder outlet obstruction (PBOO) demonstrate an increased expression of desmin, as well as the induction of vimentin expression, in bladder smooth muscle (BSM) (10, 11) Similar increases in desmin is seen in the bladder wall smooth muscles of patients with benign prostatic hyperplasia (BPH) (11). Muscle pathological changes including diminished contractility of smooth muscle in obstructed bladder suggests a role for desmin and vimentin overexpression in contributing to muscle dysfunction. However, the molecular mechanism by which desmin and vimentin contribute to BSM dysfunction is not known.

Early studies demonstrate that desmin and vimentin proteins directly participate in signal transduction (12). IFs act as scaffolds as well as regulators of signaling molecules including protein kinases (13, 14). Stretch-induced JNK signaling has been shown to be greatly reduced in desmin-deficient skeletal muscle in mice (13). Vimentin transports phosphorylated ERK1 and ERK2 from the site of axonal lesion to the nerve cell body and increased vimentin expression in injured neurons determines the stress induced ERK1/2 signaling (14) (13). Moreover, vimentin interacts with the RAF-1/RhoA signaling pathway (15, 16) to mediate actin dynamics and focal adhesion formation (17), and vimentin depletion resulted in increased myosin light chain phosphorylation (MLC_{20}) and increased contractility in human osteosarcoma and human dermal fibroblasts (18).

Previous studies have demonstrated that JNK along with its substrate c-Jun are activated in response to mechanical stretch in rodent and human BSM cells (19–21). In the current study, we transduced IF proteins into murine BSM strips via an adenovirus to examine the sufficiency of increased IF protein expression to reduce BSM contraction. Our data

demonstrate that the increased expression of desmin and vimentin in murine BSM strips decreased the peak forces in response to KCl and carbachol. This effect is associated with increased JNK2 phosphorylation and reduced MLC_{20} phosphorylation. Desmin and vimentin overexpression did not alter contractility or MLC_{20} phosphorylation in strips isolated from JNK2 knockout (KO) mice, strongly implicating JNK2 in mediating the effects of desmin and vimentin on BSM muscle contractility. Pharmacological JNK2 inhibition produced results qualitatively similar to those caused by JNK2 deficiency (KO). These findings provide compelling evidence for a negative role of IFs and JNK2 in BSM contraction.

Materials and Methods

Mice

Male C57BL/6J and JNK2 knockout (KO) mice in C57BL/6J background were purchased from Jackson Laboratory (Bar Harbor, ME, USA). All experiments were approved according to animal experimental ethics committee guidelines by the Institutional Animal Care and Use Committee at Thomas Jefferson University. For all contractility, molecular, histological and immunofluorescence studies, age matched wild type (WT) and JNK2 KO mice were used and the mice used in this study were aged between 10–11 weeks old. Mice were euthanized by CO_2 asphyxiation and at the time of sacrifice, body weight and bladder weights were recorded.

Protein extraction and immunoblot analysis

Protein was extracted and analyzed by western blotting as described previously (10). Briefly, total proteins from each sample were separated by sodium dodecyl sulfate-polyacrylamide gel electrophoresis (SDS-PAGE) and transferred to polyvinylidene difluoride membranes (Millipore, Bedford, MA). The proteins were subjected to immunoblot analysis using antibodies specific for desmin, SMA, SMHC, SM22 (Abcam, Cambridge, MA, USA), vimentin, GFP, JNK1, JNK2, phospho-JNK (Cell Signaling Technology, Danvers, MA, USA), phospho-myosin light chain (Thr18/Ser19) (Cell Signaling Technology, Danvers, MA, USA), myosin light chain (Abcam, Cambridge, MA, USA) and GAPDH (Millipore, Burlington MA, USA) antibodies. The immunoreactive proteins were visualized as described previously (10). Equal loading was confirmed by probing the membranes with anti-GAPDH antibody. Bands were quantified by densitometry using an Alpha Innotech FluroChem 8800 Image system (Protein Simple, San Jose, CA, USA). Expression of protein of interest except $pMLC_{20}$ was normalized to the expression of GAPDH. Protein bands from immunoblots for $pMLC_{20}$ were quantitated and normalized the data with MLC_{20}.

Co-immunoprecipitation analysis

The interaction of JNK2 with desmin and vimentin proteins was studied in murine BSM strips by co-immunoprecipitation (Co-IP) as described previously (22), (23) (24). Protein samples were prepared by lysing the BSM strips in lysis buffer (50 mM HEPES (pH 7.6), 150 mM NaCl, 1 mM EDTA, 1 mM EGTA, 10 mM MgCl2, 1% sodium deoxycholate, 1% Triton X-100, protease inhibitor cocktail (1:100 dilution, Sigma, St. Louis, MO), phosphatase inhibitor cocktail (1:100 dilution, Sigma, St. Louis, MO), 0.1 mM sodium

orthovanadate). The lysate was centrifuged at 20,000 x g for 20 min at 4°C and the supernatant collected. The lysate was pre-cleared by adding Dynabeads Protein A and incubating the mixture for 30 min on a rocker at 4°C. The Dynabeads were separated from the lysate using a magnetic separation rack, and the pre-cleared lysate was used for immunoprecipitation (IP) experiments. Pre-clearing the lysate was performed to reduce the non-specific binding of the proteins to the beads. The pre-cleared lysate was incubated with antibody directed against JNK1 or JNK2 in a micro centrifuge tube and the mixture was incubated with rotation overnight at 4° C to form the immunocomplex. JNK1 or JNK2 antibody used for immunoprecipitation was cross linked to the Dynabeads as per the manufacturer's instructions (Thermo Fisher Scientific, Waltham, MA) to avoid co-elution of the JNK1 or JNK2 antibody with the immunoprecipitated proteins. The antibody-antigen complex was captured by incubating the mixture with Dynabeads Protein A for 2 hr at 4°C on a rotating wheel followed by magnetic separation. After three washes with the lysis buffer, the protein-antibody complexes were eluted from the beads with 0.1 M citrate buffer (pH 2–3) followed by precipitation of the proteins with ethanol. The protein samples were immunoblotted with anti-JNK2, JNK1, desmin and vimentin antibodies.

Immunofluorescence and confocal microscopy

Frozen 5-μm sections from murine BSM strips devoid of urothelium and submucosa were mounted on a glass slide. Immunofluorescence staining of specific proteins was performed as described previously (25). Smooth muscle myosin heavy chain (SMHC) and SM22 (also known as transgelin) are well known markers of differentiated smooth muscle. In the current study, SM22 was used to determine the smooth muscle-specific localization of proteins in murine BSM. The primary antibodies used were Cy3 labelled SMA, Cy3 labelled vimentin (Sigma, Saint Louis, MO, USA), anti-rabbit SMHC, anti-goat SM22 anti-rabbit desmin (Abcam, Cambridge, MA, USA), Alexa Fluor 488 labelled GFP (Invitrogen, Carlsbad, CA, USA). The secondary antibodies used were anti-rabbit Cy3-conjugated and anti-goat Alexa Fluor 647-conjugated antibodies (Invitrogen). All samples were mounted using VectaShield mounting medium (Vector Laboratories, Inc. Burlingame, CA). High-resolution laser scanning fluorescence microscopy was performed at room temperature using a confocal microscope (Nikon NIS-Element v5.02, Nikon Instruments Inc, Melville, NY, USA).Objective lens with numerical aperture 1.45 (100× and 60x oil immersion) was used for capturing the images and images were acquired as series of Z stacks and imported into ImageJ (National Institutes of Health, Bethesda, USA) using LOCI Bio-Formats. The Cy3, fluorescein isothiocyanate (FITC), and Alexa Fluor 647 fluorescence emissions appear red, green, and blue, respectively. Fluorescence intensities of the confocal images were quantitated using FIJI ImageJ software (National Institutes of Health, Bethesda, USA).

BSM tissue preparation and transduction with adenovirus

Bladders from wild type (WT) and JNK2 KO male mice were removed carefully and placed in ice cold Tyrode buffer (120 mM NaCl, 2.7 mM KCl, 0.4 mM NaH_2PO_4, 1.8 mM $CaCl_2$, 0.5 mM $MgCl_2$, 23.8 mM $NaHCO_3$ and 5.6 mM glucose). The bladder neck, trigone, base region, the urothelium and submucosa were removed and the bladders were divided in the midsagittal plane, and cut into longitudinal strips. The bladders were cut into longitudinal strips approximately 2 mm wide and 4–5 mm long and the muscle strips were prepared for

adenovirus transduction as described previously (26). Briefly, the strips were mounted onto polymerized silicone elastomer (Dow Corning, Midland, MI, USA) using 0.1 mm stainless pins. The pins were positioned such that the strips were slightly stretched longitudinally while raised 2–3 mm above the surface of the elastomer. Muscle strips were maintained in a serum free medium composed of DMEM/F-12 (1:1 ratio, Cellgro, Mediatech, Manassas, VA, USA) supplemented with 100U/ml penicillin, 100 μg/ml streptomycin, 250 ng/ml amphotericin B, 35 μg/ml-ascorbic acid, 5 μg/ml transferrin, 3.25 ng/ml selenium, 2.85 μg/ml insulin, and 200 μg/ml glutamine and placed in a 37ºC, 5% CO_2 incubator for up to two days. Murine BSM strips were subjected to 110 mM KCl stimulation for 5 min daily for up to two days. Muscle strips were washed with sterile PSS for 10 min, prior to and after stimulation with KCl. Muscle strips were incubated with fresh serum-free medium after the sterile PSS wash. PSS contained (in mM) 140 NaCl, 4.7 KCl, 1.2 $MgSO_4$, 1.6 $CaCl_2$, 1.2 Na_2HPO_4, 2 MOPS (pH 7.4), 5 D-glucose, and 0.02 EDTA. The muscle strips were transduced with an adenovirus coding for GFP, desmin or vimentin protein for 48 h, using 10 μl of virus (titer of 10^8pfu/ml) for each strip in 500 μl medium.

Measurement of isometric force

Contractility measurements of adenovirus-transduced BSM strips from WT and JNK2 KO mice were performed as described previously (27). BSM strips were removed from silicone elastomer and attached to a force transducer and suspended in organ baths containing Tyrode buffer. Muscle strips were stretched to a force of 1.5 g. The organ baths were continually gassed with 95% O_2 and 5% CO_2 and pH of the buffer was maintained at 7.4. The bladder strips were equilibrated for approximately 60 min and the buffer was refreshed every 10 min during the equilibration time. Following equilibration, the strips were stimulated with high potassium (120 mM KCl) Tyrode buffer (7.7 mM NaCl, 120 mM KCl, 0.4 mM NaH_2PO4, 1.8 mM $CaCl_2$, 0.5 mM $MgCl_2$, 23.8 mM $NaHCO_3$, and 5.6 mM glucose) and change in tension was recorded. The strips were washed four times with fresh Tyrode buffer after KCl stimulation. Following equilibration, strips were stimulated with cholinergic receptor agonist, carbachol (cumulative addition from 10^{-9} to 3×10^{-5} M). Isometric contractions were measured by the force transducers and recorded with the bridge amplifier connected to an analog-to-digital converter (AD Instruments, Inc. Colorado Springs, CO, USA) and the data was analyzed by Lab Chart 7 Software. The force measurements were normalized to the cross-sectional area (grams/mm^2) of the muscle strips.

Measurement of MLC_{20} phosphorylation

MLC_{20} phosphorylation in BSM strips was measured as described previously (28). Briefly, BSM strips removed from silicone elastomer were suspended in organ baths containing Tyrode buffer and stretched to generate a force of 1.5 g. Following equilibration, the strips were stimulated with either high potassium (120 mM KCl) or carbachol (10 μM) and then frozen rapidly by clamp-freezing in liquid nitrogen, followed by immersion in a dry ice/acetone slurry containing 10% trichloroacetic acid (TCA) and 10 mM DTT. The strips were slowly thawed at room temperature, washed in acetone, air dried, and then subjected to homogenization and precipitated the protein in 10% TCA with 10 mM DTT. The samples were centrifuged at 12,000 rpm for 10 min and the protein pellet was washed with diethylehter, air-dried and resuspended in sample buffer. Equal amounts of proteins were

resolved on SDS-PAGE and transferred to polyvinylidene difluoride membranes (Millipore, Bedford, MA). The proteins were subjected to immunoblot analysis using phospho-myosin light chain (Thr18/Ser19) (Cell Signaling Technology, Danvers, MA, USA) and myosin light chain antibodies (Abcam, Cambridge, MA, USA).

Histology

Age-matched WT and JNK2 KO mice were used for histological studies. After euthanasia, WT and JNK2 KO murine bladders were fixed in 10% neutral buffered formalin at room temperature. The fixed bladder tissue from WT and JNK2 KO mice was paraffin-embedded and five μm thick sections were stained with Masson's trichrome stain (MTS) using standard techniques. MTS stained bladder sections were imaged using a Light Microscope BX43 (Olympus, Waltham, MA, USA). Paraffin embedded bladder sections from WT and JNK2 KO mice were subjected to deparaffinization and rehydration using xylene and ethanol. Antigen unmasking was performed using antigen retrieval buffer (Abcam, Cambridge, MA, USA) as per the manufacturer's instructions. For immunofluorescence staining, BSM strips overexpressing desmin, vimentin and GFP were embedded in optimal cutting temperature compound (OCT: Sakura, Tokyo, Japan) and frozen with liquid nitrogen for cryo-sectioning. A series of adjacent sections were cut on a cryostat. Each section with 5 μM thickness was mounted onto a charged slide.

JNK2 inhibitor studies

The JNK2 inhibitor IX (Cayman Chemicals, Ann Arbor, MI) is a thienylnaphthamide compound that targets the ATP binding site of JNK2 and JNK3; it is highly selective for JNK2 and JNK3 with very little activity against JNK1 and other MAP kinases (29). Preliminary studies examining the dose-dependent effect of JNK2 inhibitor IX (JNK2-IX) in BSM strips established 100 nM as the optimum concentration for the inhibition of pJNK levels (data not shown). Accordingly, murine BSM strips were treated with 100 nM JNK2-IX for 48 h prior to analysis of contractile regulation.

Statistical Analysis

Statistical analyses were performed using Prism 7 (GraphPad Software, La Jolla, CA). For comparisons between two-group means, Student t-test was performed. For comparison between more than two groups ANOVA was performed with post hoc Bonferroni pair wise comparisons. A p value of < 0.05 or < 0.01 was considered significant for all analyses. Data are presented as the mean ± standard error of the mean (SEM) or SD. The value of n is equal to the number of mice from which strips were obtained

Results

Adenovirus-mediated overexpression of desmin and vimentin in murine BSM strips

Schematic representation of desmin-GFP and vimentin-GFP bicistronic adenoviral vector is shown in Fig. 1A and 2A respectively. Schematic representation of GFP adenoviral vector is shown in Fig 1B and 2B. Transduction of murine BSM strips with an adenoviral vector encoding desmin or vimentin for 48 h resulted in up-regulation of desmin (3 fold) and vimentin (3.5 fold) proteins respectively relative to the level in GFP-expressing murine BSM

strips (Fig. 1C and 2C). Interestingly, there was a significant increase in vimentin protein expression (2.5-fold) in desmin-overexpressing murine BSM strips relative to the level of GFP expressing murine BSM strips (Fig. 1D). Conversely, vimentin overexpression did not alter the expression of desmin in murine BSM strips (Fig. 2D). The relative intensities of the bands for desmin and vimentin in Fig. 1C and D and in Fig. 2C and D were quantified and normalized to GAPDH (Fig 1E-F and 2E-F). Sections from murine BSM strips overexpressing GFP, desmin, or vimentin were stained with antibodies specific for GFP, desmin or vimentin and examined by confocal microscopy. Representative confocal images are shown in Fig. 1G & 2G. Desmin and vimentin protein expression was significantly increased in desmin and vimentin overexpressing murine BSM strips respectively relative to the level in GFP- expressing murine BSM strips (Fig. 1G–H and 2G–H). The increased expression of desmin and vimentin specifically within the smooth muscle was further confirmed by co-staining the tissue section with smooth muscle marker protein SM22 (Fig. 1G & 2G). We observed vimentin expression in non-muscle cells in murine BSM strips expressing GFP and these cells are present in between the smooth muscle bundles (Fig 2G). Vimentin positive cells were also observed along the edges of SM22 positive SMCs (Fig 2G).

Co-localization of desmin and vimentin in murine BSM strips overexpressing desmin

Localization of desmin and vimentin IFs proteins in murine BSM strips overexpressing desmin was studied by double label immunofluorescence microscopy. Representative confocal images are shown in Fig. 3. Desmin overexpression induced vimentin expression in the smooth muscle cells. Vimentin expression appears to occur in the same smooth muscle cells where desmin is present.

Increased expression of desmin and vimentin reduces murine BSM contraction

To determine the contractile properties of BSM strips overexpressing GFP, desmin or vimentin we measured the force generation in these strips in response to KCl or carbachol. Desmin and vimentin overexpression decreased the peak forces developed in response to 120 mM KCl (Fig 4A) and carbachol (Fig. 5A) relative to the tension developed in GFP-expressing murine BSM strips (Fig. 4A and 5A). Desmin overexpression decreased the contractile force in response to KCl and carbachol stimulation by over 50% relative to the force of GFP-expressing murine BSM strips (Fig. 4A-B and 5A). Vimentin overexpression decreased the contractile force in response to KCl and carbachol stimulation by over 70% relative to the force of GFP-expressing murine BSM strips (Fig. 4A–B and 5A). Overexpression of GFP in murine BSM strips did not alter the force relative to the level of uninfected murine BSM strips (without GFP expression) in response to KCl and carbachol (Fig. 4B & 5B). Collectively, these results demonstrate that increased desmin and vimentin expression decreases depolarization-induced and agonist-mediated smooth muscle contraction in murine bladder.

Increased expression of desmin and vimentin reduces MLC_{20} phosphorylation in murine BSM

MLC_{20} phosphorylation is one of the determinants of smooth muscle contraction (30). MLC phosphorylation levels are determined by the balance between MLC kinase and MLC

phosphatase activities (31). MLC_{20} phosphorylation of BSM strips at resting tension and with KCl (120 mM) or carbachol (10 μM) stimulation was determined by immunoblot analysis, and representative immunoblots are shown in Fig 4C–F and Fig 5C–F. Stimulation with KCl or carbachol of BSM strips overexpressing GFP increased phospho MLC_{20} levels. However, increased expression of desmin or vimentin significantly reduced MLC_{20} phosphorylation levels induced by KCl or carbachol (4C-F & Fig 5C–F). Overexpression of desmin or vimentin in murine BSM strips did not significantly alter the resting levels of phospho MLC_{20} relative to the level in GFP-expressing BSM strips (4C–D & Fig 5C–D).

Effect of desmin and vimentin overexpression on smooth muscle marker proteins expression in murine BSM

Total proteins and tissue sections obtained from GFP-, desmin- and vimentin-overexpressing murine BSM strips were subjected to immunoblot analysis for SMA and SM22 and for immunofluorescence analysis of SMHC, SM22 and SMA respectively. Overexpression of desmin and vimentin in murine BSM strips did not significantly alter the levels of SMA, SM22 and SMHC proteins relative to the level of GFP expressing murine BSM strips (Fig. 6A–E & Fig 7A–E). For unknown reason, the overexpression of either desmin or vimentin did not alter the smooth muscle markers, such as SM22, SMHC and α-SMA protein expression in murine BSM.

Desmin and vimentin interact with JNK2 following IF protein overexpression in murine BSM

IF proteins are known to interact with protein kinases (12, 14). IF proteins act as a scaffold for the protein kinases and enhance their signaling (13, 14, 32–34). The JNK family was shown to be the most relevant among three subsets of MAPK family members being activated in response to mechanical stretch in rodents and human BSM cells (19–21). Therefore, we determined whether JNK isoforms interact with desmin or vimentin following IF protein overexpression. JNK isoforms were immunoprecipitated from cell lysates with JNK1 or JNK2 antibody following IF protein overexpression and the immunoprecipitated proteins were subjected to immunoblot analysis with anti-desmin or anti-vimentin antibody. As shown in Figure 8A–B**,** JNK2 antibody immunoprecipitated the desmin and vimentin following the IF protein overexpression in murine BSM strips. However, the JNK1 antibody failed to pull down desmin or vimentin from GFP, desmin or vimentin overexpressing murine BSM strips (Fig S1). Collectively these results demonstrate that desmin and vimentin interact with JNK2 when the IF proteins are overexpressed in murine BSM.

Increased expression of desmin and vimentin enhances JNK phosphorylation in murine BSM

We next investigated the effect of desmin and vimentin overexpression on JNK phosphorylation in murine BSM strips. The phosphorylation status of JNK was determined by immunoblotting with an antibody which specifically recognizes dual phosphorylated TPY motif in the activation loop. GFP-expressing murine BSM strips were used as a control for the basal JNK phosphorylation. Immunoblot analyses showed that the overexpression of

desmin and vimentin in murine BSM strips increased JNK phosphorylation relative to the level in GFP-expressing murine BSM strips (Fig. 8C–F).

JNK2-deficient mice exhibit increased BSM mass and enhanced contractile proteins expression

Immunoblot analysis demonstrated the absence of JNK2 protein in BSM tissue from JNK2 KO mice (Fig. 9A). JNK2 KO mice did not show any significant difference in body weight; however, they exhibited increased bladder weights and bladder/body weight ratio compared with WT. mice (Fig. 9B–C). Masson's trichrome staining analysis of bladders from WT and JNK2 KO mice revealed a significant increase in muscle thickness within the cross section of the bladder wall in JNK2 KO mice compared with WT mice (Fig 9D–E). The immunoblot and immunofluorescence analysis revealed an increased expression of SMA, SMHC and SM22 proteins in BSM from JNK2 KO mice compared with WT mice (Fig 10A–D).

Desmin and vimentin overexpression does not alter BSM contraction in JNK2 KO mice

We measured the contractile properties of BSM strips from JNK2 KO mice overexpressing GFP, desmin or vimentin protein. Desmin and vimentin overexpression decreased the peak force developed by BSM strips from WT mice in response to KCl and carbachol relative to the force developed by GFP expressing murine BSM strips from WT mice (Fig. 4A–B and 5A). However, the resting tension (basal) as well as KCl- and carbachol-induced contractile responses were not attenuated in the BSM strips from JNK2 KO mice following desmin and vimentin overexpression relative to the levels in GFP- overexpressing BSM strips from JNK2 KO mice (Fig. 11A–B and 12A–B). BSM strips from JNK2 KO mice showed increased peak force relative to the peak force developed by BSM strips from WT mice in response to KCl and carbachol (Fig 11C and 12C).

Desmin and vimentin overexpression does not alter MLC_{20} phosphorylation in BSM from JNK2 KO mice

MLC_{20} phosphorylation of BSM strips from WT and JNK2 KO mice overexpressing GFP, desmin or vimentin proteins at the resting tension and with KCl (120 mM) or carbachol (10 μM) stimulation was determined by immunoblot analysis and the representative immunoblot is shown in Fig 11D–E and 12D-E. The resting levels as well as the KCl- and carbachol-induced MLC_{20} phosphorylation were not attenuated in the BSM strips overexpressing desmin or vimentin from JNK2 KO mice relative to the levels in GFP- overexpressing BSM strips from JNK2 KO mice (Fig 11F–G and 12F–G). BSM strips from JNK2 KO mice showed increased MLC_{20} phosphorylation relative to the level in BSM strips from WT mice in response to KCl and carbachol stimulation (Fig 11E & H and 12E & H). BSM strips from JNK2 KO mice did not show any change in the resting (basal) MLC_{20} phosphorylation relative to its level in BSM strips from WT mice (Fig 11E and 12E).

Pharmacological inhibition of JNK2 activity rescues the decreased contractile responses as well as the decrease in MLC_{20} phosphorylation observed with desmin or vimentin overexpression in murine BSM

To investigate the effects of pharmacological JNK2 inhibition on IFs proteins overexpression induced JNK2 phosphorylation, we treated the murine BSM strips overexpressing GFP, desmin or vimentin with JNK2 inhibitor-IX for 48 h. Immunoblot analyses showed that treatment of murine BSM strips overexpressing desmin and vimentin with JNK2 inhibitor-IX (100 nM) for 48 h substantially reduced the level of phospho JNK2 (Fig 13A–F) without altering the JNK2 protein expression levels.

To complement the JNK2 KO mice study, we measured the contractile properties and MLC_{20} phosphorylation of murine BSM strips overexpressing GFP, desmin or vimentin in the presence or absence of JNK2 inhibitor-IX in response to KCl or carbachol stimulation. Treatment with 100 nM JNK2 inhibitor-IX rescued the decreased contractile responses as well as the decrease in MLC_{20} phosphorylation observed with desmin or vimentin overexpression in response to KCl and carbachol stimulation (Fig 14 A–E and 15A–D). However, MLC_{20} phosphorylation at the resting tension was not attenuated in the BSM strips overexpressing desmin or vimentin in the presence or absence of JNK2 inhibitor-IX relative to the levels in GFP-overexpressing BSM strips (Fig 14C-D and 15C). Collectively our results employing pharmacological JNK2 inhibition and genetic deletion of JNK2 suggest that desmin and vimentin elicited their effects on muscle contractility via JNK2.

Discussion

In this study, we provide the first demonstration of a role for the IF proteins desmin and vimentin in the regulation of BSM contraction. Murine BSM strips overexpressing desmin or vimentin protein displayed decreased contractility *ex vivo* and reduced MLC_{20} phosphorylation in response to either membrane depolarization (KCl) or the cholinergic agonist carbachol compared with murine BSM strips expressing GFP. Furthermore, we demonstrate that the overexpression of desmin and vimentin in BSM strips from JNK2 KO mice did not attenuate the KCl- and carbachol-induced contraction as well as MLC_{20} phosphorylation relative to the levels in GFP-overexpressing BSM strips from JNK2 KO mice. Pharmacological JNK2 inhibition produced results qualitatively similar to those caused by JNK2 KO. Mechanistically, the effect of desmin or vimentin overexpression in reducing BSM contractility was associated with a reduction in induced $pMLC_{20}$ levels, an effect absent in JNK2 KO mice.

Smooth muscle contraction is regulated by a network of signaling pathways centered on myosin as well as membrane properties associated with calcium handling. Depolarization of the cell membrane activates voltage gated Ca^{2+} -channels resulting in Ca^{2+} influx and activation of myosin cross bridge cycling on actin filaments and myosin phosphorylation (MLC_{20}) catalyzed by Ca^{2+} calmodulin dependent MLCK. MLC_{20} phosphorylation and muscle force is maintained by several signaling pathways including Ca^{2+} independent kinases, and inhibition of myosin phosphatase (35, 36). However, recent findings highlighted the importance of the actin cytoskeleton and IF proteins in active force development in smooth muscle contraction (37–40). An earlier study by Wang et al., demonstrated that a

deficiency of the IF protein vimentin attenuates the contractile responses of airway smooth muscle to agonist stimulation (40). Vimentin depletion by antisense oligonucleotide in airway smooth muscle strips isolated from canine trachea suppressed contractile responses to acetylcholine (8, 40). These studies suggest that vimentin plays an important role in mediating the active force development in airway smooth muscle. Contrary to the effect of vimentin knockdown reported in airway smooth muscle by Wang et al., in the current study, murine BSM strips overexpressing vimentin protein generated less force when stimulated with cholinergic agonist or in response to membrane depolarization compared with GFP-expressing murine BSM strips. This difference may be because vimentin is not expressed in normal murine BSM.

Desmin IF protein has a role in the intracellular transmission of active force in smooth muscle possibly by alignment of contractile units and cell to cell or cell-matrix coupling (2, 41). Previous studies have demonstrated that desmin is essential for both active and passive force transmission in smooth muscle (2, 41). Interestingly Scott et al. demonstrated that BSM from obstructed mice produced lower active force than sham operated control mice and the BSM from obstructed desmin KO mice did not show any difference in active force generation compared with sham operated control WT mice (2). Findings from these studies suggest that the increase in desmin expression during hypertrophy in WT mice contributes to the loss of active force (2). In the current study, murine BSM strips overexpressing desmin protein displayed diminished contractility when stimulated with cholinergic agonist or in response to membrane depolarization. Furthermore, diminished contractility of murine BSM strips following desmin overexpression was associated with an increased expression of vimentin. It is possible that the increased vimentin expression in these strips contributes to the diminished contractility in response to KCl and carbachol.

It is well-established that smooth muscle cross bridge cycling is regulated by phosphorylation of the MLC_{20} (42). MLC_{20} phosphorylation plays an important role in the initial development of smooth muscle contraction (43) (44). Murine BSM strips overexpressing desmin or vimentin displayed a significant reduction in MLC_{20} phosphorylation and decreased force generation in response to K^+-depolarization and carbachol stimulation suggesting an essential role of desmin and vimentin in depolarization- and cholinergic agonist-mediated contraction of BSM possibly via MLC_{20} phosphorylation. MLC_{20} phosphorylation was not attenuated in the BSM strips overexpressing desmin or vimentin from JNK2 KO mice relative to the levels in GFP-overexpressing BSM strips from JNK2 KO mice. This is further confirmed by the pharmacological inhibition of JNK2 activity, as reducing the phospho JNK2 level by JNK2 inhibitor IX in murine BSM strips overexpressing desmin or vimentin rescued the decreased contractile responses and the decrease in MLC_{20} phosphorylation observed with desmin and vimentin overexpression.

Previous studies have shown that JNK2 signaling can control smooth muscle contractility as well as various pathological states in different tissues. An early study by Laukeviciene et al. demonstrated that ablation of either JNK2 gene or JNK3 gene did not alter the contractility of small blood vessels in carotid arteries in response to KCl or histamine stimulation. However, silencing of both JNK2 and JNK3 genes in mice (double knockout) resulted in increased contractility of small blood vessels in carotid arteries compared to wild type or

single knockout in response to KCl or phenylephrine or noradrenaline stimulation (45). The JNK inhibitor CC-930 attenuated lung remodeling and collagen deposition and other pulmonary fibrotic systemic markers in house dust mite-induced fibrotic airway mouse model (46). JNK1 and JNK2 KO mice were protected against hypercholesterolemia induced endothelial dysfunction and atheroma formation (47–49). The contribution of JNK2 signaling to muscle remodeling is increasingly appreciated (50). In the current study, we examined the role of JNK2 signaling in BSM contraction. We demonstrate for the first time that BSM strips from JNK2 KO mice produced more force in response to KCl or carbachol relative to the level in WT murine BSM strips. Contrary to findings in small blood vessels in carotid artery (45), we show that in murine bladder smooth muscle, genetic deletion of the JNK2 gene increases contractility. One potential explanation for the differing results of Laukeviciene et al. may be due to the redundancy of JNK isoform function in carotid arteries. We did not detect JNK3 expression in murine BSM strips. In the current study, although mechanistic insights that explain the increased contractility of BSM of JNK2 KO mice in response to KCl and carbachol remains unclear, a role for MLC_{20} phosphorylation seems likely.

Earlier studies have shown that IFs directly participate in protein kinase signaling (13, 14). For example, isolated skeletal muscle tissue from desmin KO mice did not induce JNK phosphorylation when the tissue was subjected to stretch, whereas stretch of the skeletal muscle tissue from WT mice strongly phosphorylated both 54 kDa and 46 kDa isoforms of JNK (13). These findings from desmin KO mice demonstrate that JNK-mediated stress signaling in skeletal muscle is mediated through desmin (13) ~~50~~). In our study, we demonstrate for the first time that desmin interacts with JNK2 and increases JNK phosphorylation following the IF protein desmin overexpression in murine BSM.

Diminished BSM contractility stems from various conditions afflicting the lower urinary tract including the lower urinary tract symptoms associated with bladder outlet obstruction (51). Our findings suggest JNK2 as a major effector of IF protein overexpression-induced BSM contractile dysfunction. Further, our data implicate an IFs/JNK2 dependent mechanism that contributes to the pathologic bladder contractility that occurs following bladder outlet obstruction, a condition in which desmin and vimentin protein expression is known to be up-regulated (10, 11). Together, these findings suggest that desmin-JNK2 and vimentin-JNK2 axes are likely to contribute to diminished BSM contractility associated with obstructive bladder disease and that JNK2 inhibition may have therapeutic application.

Localization of endogenous vimentin and desmin in smooth muscle cells of large arteries and tunica media from different species including humans (52) (53) (54) demonstrated that desmin and vimentin exhibited intense cytoplasmic staining and thicker structures (52). In the current study, desmin and vimentin IFs exhibited intense cytoplasmic staining and thicker filamentous structures in murine BSM strips overexpressing desmin or vimentin which is similar to the *endogenous* vimentin and desmin staining pattern in smooth muscle cells of large arteries and in tunica media reported by Schmid et al. (52) and others (53) (54).

An early study by Despa et al., (55) demonstrated that amylin oligomers attach to the sarcolemma causes myocyte Ca^{2+} dysregulation, pathological remodeling and diastolic

dysfunction in a rat model of hyperamylinemia transgenic for human amylin (55). Further, Gianni et al., demonstrated that oligomeric protein aggregates promote an increase in systolic [Ca^{2+}] that altered Ca^{2+} homeostasis and induced cardiac contractile dysfunction implicating protein aggregates as a significant driver of signaling (56). Since IF proteins are prone to aggregation, in the current study, we speculate that some of the intense desmin and vimentin staining observed in the immunofluorescence in murine BSM strips overexpressing desmin or vimentin might be due to aggregation. However, the possible protein aggregates formed in these tissues did not impair desmin and vimentin staining pattern and the filamentous structures. The staining pattern and the filamentous structure observed in these tissues are very much similar to the endogenous vimentin and desmin staining pattern and the filamentous structures in smooth muscle cells of large arteries and in tunica media reported by Schmid et al. and others (52) (53) (54), therefore, in the current study it is unlikely that the possible protein aggregates formed in these BSM strips significantly affects the signaling.

Smooth muscle myosin heavy chain (SMHC) is a major component of thick filaments of the contractile apparatus and it is exclusively expressed in smooth muscle (57). SMHC shows the highest degree of cell specificity of any known markers of differentiated smooth muscle (58). Alpha smooth muscle actin (α-SMA) is a monomeric subunit of thin filaments that form part of the contractile machinery. Although SMA is transiently expressed during development in other mesoderm derived tissues (59) and in myofibroblasts during wound repair (60), it is normally expressed only in smooth muscle and smooth muscle cells-like cells in the adult (53). SM22, also known as transgelin, is a 22 kDa, smooth muscle cell lineage-restricted protein that is abundantly and exclusively expressed in visceral and vascular smooth muscle cells during postnatal development (61). SM22 associates with actin thin filament bundles in contractile smooth muscle (62). The exact function of SM22 in smooth muscle, however, is not known. Various studies have shown that vimentin is mainly expressed in undifferentiated and proliferative cells of mesenchymal origin and upon differentiation, it is replaced by desmin in cardiac and visceral smooth muscle (63) (64) (65). In agreement with its role in proliferation, overexpression of the vimentin gene in transgenic mice inhibits normal lens cell differentiation (66). In the current study, desmin overexpression induced vimentin expression in smooth muscle. Based on all the above findings, it is expected that desmin or vimentin overexpression should reduce the smooth muscle markers expression. However, for unknown reason the overexpression of either desmin or vimentin did not alter the smooth muscle markers, such as SM22, SMHC and α-SMA protein expression in murine BSM.

In summary, this is the first report that demonstrates that desmin and vimentin overexpression reduces murine BSM contraction, increases JNK phosphorylation and reduces MLC_{20} phosphorylation. Mechanistically, the effect of desmin or vimentin overexpression in reducing BSM contractility was associated with a reduction in induced $pMLC_{20}$ levels, an effect absent in JNK2 KO mice. This study has some limitations. Most importantly, we failed to inactivate the vimentin protein or deplete the vimentin expression in murine BSM strips overexpressing desmin. This approach would have helped to explain whether the overexpression of either desmin or vimentin is interchangeable or they elicit different response in murine BSM. There are no effective oral drugs available to improve

detrusor contractility in underactive bladder. The use of cholinergic receptor agonists or anticholinesterases to augment bladder contractility or α adrenoceptor antagonists to reduce bladder outlet resistance did not significantly improve contraction in patients with impaired detrusor contractility (67) highlighting the need to identify novel therapeutic targets for pharmacological treatment of underactive bladder. To date, JNK inhibition has been explored as a possible anticancer and arthritis therapeutic target in clinical trials. Our results provide important guidelines for exploring therapeutic strategies of JNK inhibition to address bladder contractile dysfunction, an attractive and still unexplored option.

Supplementary Material

Refer to Web version on PubMed Central for supplementary material.

Acknowledgments

The study was funded by the U.S. National Institute of Health (NIH) National Institute of Diabetes and Digestive and Kidney Diseases (R01 grant DK100483 to Boopathi Ettickan and R01grant NIDDK035385 to Satish Rattan). The content is solely the responsibility of the authors and does not necessarily represent the official views of the NIH.

Abbreviations

IFs	intermediate filaments
IF	intermediate filament
BSM	bladder smooth muscle
WT	wild type
KO	knockout
PBOO	partial bladder outlet obstruction
BPH	benign prostatic hyperplasia
MTS	Masson’s trichrome stain
SEM	Standard error mean
ERK2	Extracellular Signal-Regulated Kinase
JNK2	c-Jun N-terminal kinase (JNK)
JNK2-IX	JNK2 inhibitor IX
SMHC	Smooth muscle myosin heavy chain
SMA	smooth muscle actin
SM22	smooth muscle protein 22
MLC	Myosin light chain

pMLC	Phospho myosin light chain

Bibliography

1. Capetanaki Y, Bloch RJ, Kouloumenta A, Mavroidis M, and Psarras S (2007) Muscle intermediate filaments and their links to membranes and membranous organelles. Exp Cell Res 313, 2063–2076 [PubMed: 17509566]
2. Scott RS, Li Z, Paulin D, Uvelius B, Small JV, and Arner A (2008) Role of desmin in active force transmission and maintenance of structure during growth of urinary bladder. Am J Physiol Cell Physiol 295, C324–331 [PubMed: 18562479]
3. Fletcher DA, and Mullins RD (2010) Cell mechanics and the cytoskeleton. Nature 463, 485–492 [PubMed: 20110992]
4. Lowery J, Kuczmarski ER, Herrmann H, and Goldman RD (2015) Intermediate Filaments Play a Pivotal Role in Regulating Cell Architecture and Function. J Biol Chem 290, 17145–17153
5. Eriksson JE, Opal P, and Goldman RD (1992) Intermediate filament dynamics. Curr Opin Cell Biol 4, 99–104 [PubMed: 1558758]
6. Chang L, and Goldman RD (2004) Intermediate filaments mediate cytoskeletal crosstalk. Nat Rev Mol Cell Biol 5, 601–613 [PubMed: 15366704]
7. Draeger A, Amos WB, Ikebe M, and Small JV (1990) The cytoskeletal and contractile apparatus of smooth muscle: contraction bands and segmentation of the contractile elements. J Cell Biol 111, 2463–2473 [PubMed: 2277068]
8. Tang DD (2008) Intermediate filaments in smooth muscle. Am J Physiol Cell Physiol 294, C869–878 [PubMed: 18256275]
9. Quinlan RA, and Franke WW (1982) Heteropolymer filaments of vimentin and desmin in vascular smooth muscle tissue and cultured baby hamster kidney cells demonstrated by chemical crosslinking. Proc Natl Acad Sci U S A 79, 3452–3456 [PubMed: 6954489]
10. Polyak E, Boopathi E, Mohanan S, Deng M, Zderic SA, Wein AJ, and Chacko S (2009) Alterations in caveolin expression and ultrastructure after bladder smooth muscle hypertrophy. J Urol 182, 2497–2503 [PubMed: 19765744]
11. Malmqvist U, Arner A, and Uvelius B (1991) Cytoskeletal and contractile proteins in detrusor smooth muscle from bladders with outlet obstruction--a comparative study in rat and man. Scand J Urol Nephrol 25, 261–267 [PubMed: 1723535]
12. Helfand BT, Chou YH, Shumaker DK, and Goldman RD (2005) Intermediate filament proteins participate in signal transduction. Trends Cell Biol 15, 568–570 [PubMed: 16213139]
13. Palmisano MG, Bremner SN, Hornberger TA, Meyer GA, Domenighetti AA, Shah SB, Kiss B, Kellermayer M, Ryan AF, and Lieber RL (2015) Skeletal muscle intermediate filaments form a stress-transmitting and stress-signaling network. J Cell Sci 128, 219–224 [PubMed: 25413344]
14. Perlson E, Hanz S, Ben-Yaakov K, Segal-Ruder Y, Seger R, and Fainzilber M (2005) Vimentin-dependent spatial translocation of an activated MAP kinase in injured nerve. Neuron 45, 715–726 [PubMed: 15748847]
15. Ehrenreiter K, Piazzolla D, Velamoor V, Sobczak I, Small JV, Takeda J, Leung T, and Baccarini M (2005) Raf-1 regulates Rho signaling and cell migration. J Cell Biol 168, 955–964 [PubMed: 15753127]
16. Janosch P, Kieser A, Eulitz M, Lovric J, Sauer G, Reichert M, Gounari F, Buscher D, Baccarini M, Mischak H, and Kolch W (2000) The Raf-1 kinase associates with vimentin kinases and regulates the structure of vimentin filaments. FASEB J 14, 2008–2021 [PubMed: 11023985]
17. Amano M, Fukata Y, and Kaibuchi K (2000) Regulation and functions of Rho-associated kinase. Exp Cell Res 261, 44–51 [PubMed: 11082274]
18. Jiu Y, Peranen J, Schaible N, Cheng F, Eriksson JE, Krishnan R, and Lappalainen P (2017) Vimentin intermediate filaments control actin stress fiber assembly through GEF-H1 and RhoA. J Cell Sci 130, 892–902 [PubMed: 28096473]

19. Kushida N, Kabuyama Y, Yamaguchi O, and Homma Y (2001) Essential role for extracellular Ca(2+) in JNK activation by mechanical stretch in bladder smooth muscle cells. Am J Physiol Cell Physiol 281, C1165–1172 [PubMed: 11546652]
20. Adam RM, Eaton SH, Estrada C, Nimgaonkar A, Shih SC, Smith LE, Kohane IS, Bagli D, and Freeman MR (2004) Mechanical stretch is a highly selective regulator of gene expression in human bladder smooth muscle cells. Physiol Genomics 20, 36–44 [PubMed: 15467014]
21. Nguyen HT, Adam RM, Bride SH, Park JM, Peters CA, and Freeman MR (2000) Cyclic stretch activates p38 SAPK2-, ErbB2-, and AT1-dependent signaling in bladder smooth muscle cells. Am J Physiol Cell Physiol 279, C1155–1167
22. Anderson DJ, and Blobel G (1983) Immunoprecipitation of proteins from cell-free translations. Methods Enzymol 96, 111–120 [PubMed: 6361451]
23. Ridge KM, Shumaker D, Robert A, Hookway C, Gelfand VI, Janmey PA, Lowery J, Guo M, Weitz DA, Kuczmarski E, and Goldman RD (2016) Methods for Determining the Cellular Functions of Vimentin Intermediate Filaments. Methods Enzymol 568, 389–426 [PubMed: 26795478]
24. dos Santos G, Rogel MR, Baker MA, Troken JR, Urich D, Morales-Nebreda L, Sennello JA, Kutuzov MA, Sitikov A, Davis JM, Lam AP, Cheresh P, Kamp D, Shumaker DK, Budinger GR, and Ridge KM (2015) Vimentin regulates activation of the NLRP3 inflammasome. Nat Commun 6, 6574 [PubMed: 25762200]
25. Zhang EY, Stein R, Chang S, Zheng Y, Zderic SA, Wein AJ, and Chacko S (2004) Smooth muscle hypertrophy following partial bladder outlet obstruction is associated with overexpression of non-muscle caldesmon. Am J Pathol 164, 601–612 [PubMed: 14742265]
26. Wang T, Kendig DM, Chang S, Trappanese DM, Chacko S, and Moreland RS (2012) Bladder smooth muscle organ culture preparation maintains the contractile phenotype. Am J Physiol Renal Physiol 303, F1382–1397
27. Lamarre NS, Braverman AS, Malykhina AP, Barbe MF, and Ruggieri MR Sr. (2014) Alterations in nerve-evoked bladder contractions in a coronavirus-induced mouse model of multiple sclerosis. PLoS One 9, e109314
28. Hypolite JA, DiSanto ME, Zheng Y, Chang S, Wein AJ, and Chacko S (2001) Regional variation in myosin isoforms and phosphorylation at the resting tone in urinary bladder smooth muscle. Am J Physiol Cell Physiol 280, C254–264 [PubMed: 11208519]
29. Angell RM, Atkinson FL, Brown MJ, Chuang TT, Christopher JA, Cichy-Knight M, Dunn AK, Hightower KE, Malkakorpi S, Musgrave JR, Neu M, Rowland P, Shea RL, Smith JL, Somers DO, Thomas SA, Thompson G, and Wang R (2007) N-(3-Cyano-4,5,6,7-tetrahydro-1-benzothien-2-yl)amides as potent, selective, inhibitors of JNK2 and JNK3. Bioorg Med Chem Lett 17, 1296–1301 [PubMed: 17194588]
30. Dillon PF, Aksoy MO, Driska SP, and Murphy RA (1981) Myosin phosphorylation and the cross-bridge cycle in arterial smooth muscle. Science 211, 495–497 [PubMed: 6893872]
31. Somlyo AP, and Somlyo AV (1994) Signal transduction and regulation in smooth muscle. Nature 372, 231–236 [PubMed: 7969467]
32. Perlson E, Michaelevski I, Kowalsman N, Ben-Yaakov K, Shaked M, Seger R, Eisenstein M, and Fainzilber M (2006) Vimentin binding to phosphorylated Erk sterically hinders enzymatic dephosphorylation of the kinase. J Mol Biol 364, 938–944 [PubMed: 17046786]
33. Kumar N, Robidoux J, Daniel KW, Guzman G, Floering LM, and Collins S (2007) Requirement of vimentin filament assembly for beta3-adrenergic receptor activation of ERK MAP kinase and lipolysis. J Biol Chem 282, 9244–9250 [PubMed: 17251187]
34. Kim S, and Coulombe PA (2007) Intermediate filament scaffolds fulfill mechanical, organizational, and signaling functions in the cytoplasm. Genes Dev 21, 1581–1597 [PubMed: 17606637]
35. Adelstein RS, and Eisenberg E (1980) Regulation and kinetics of the actin-myosin-ATP interaction. Annu Rev Biochem 49, 921–956 [PubMed: 6447472]
36. Somlyo AP, and Somlyo AV (2000) Signal transduction by G-proteins, rho-kinase and protein phosphatase to smooth muscle and non-muscle myosin II. J Physiol 522 **Pt** 2, 177–185 [PubMed: 10639096] **Pt**

37. Tang DD, and Gunst SJ (2004) The small GTPase Cdc42 regulates actin polymerization and tension development during contractile stimulation of smooth muscle. J Biol Chem 279, 51722–51728

38. Tang DD (2015) Critical role of actin-associated proteins in smooth muscle contraction, cell proliferation, airway hyperresponsiveness and airway remodeling. Respir Res 16, 134 [PubMed: 26517982]

39. Gunst SJ, Tang DD, and Opazo Saez A (2003) Cytoskeletal remodeling of the airway smooth muscle cell: a mechanism for adaptation to mechanical forces in the lung. Respir Physiol Neurobiol 137, 151–168 [PubMed: 14516723]

40. Wang R, Li Q, and Tang DD (2006) Role of vimentin in smooth muscle force development. Am J Physiol Cell Physiol 291, C483–489 [PubMed: 16571866]

41. Sjuve R, Arner A, Li Z, Mies B, Paulin D, Schmittner M, and Small JV (1998) Mechanical alterations in smooth muscle from mice lacking desmin. J Muscle Res Cell Motil 19, 415–429 [PubMed: 9635284]

42. Arner A, and Pfitzer G (1999) Regulation of cross-bridge cycling by Ca2+ in smooth muscle. Rev Physiol Biochem Pharmacol 134, 63–146 [PubMed: 10087908]

43. Kamm KE, and Stull JT (2001) Dedicated myosin light chain kinases with diverse cellular functions. J Biol Chem 276, 4527–4530 [PubMed: 11096123]

44. Somlyo AP, and Somlyo AV (2003) Ca2+ sensitivity of smooth muscle and nonmuscle myosin II: modulated by G proteins, kinases, and myosin phosphatase. Physiol Rev 83, 1325–1358 [PubMed: 14506307]

45. Laukeviciene A, Brecht S, Kevelaitis E, and Herdegen T (2006) Enhanced contractility of small blood vessels in JNK knockout mice. Eur J Pharm Sci 29, 335–339 [PubMed: 16949803]

46. van der Velden JL, Ye Y, Nolin JD, Hoffman SM, Chapman DG, Lahue KG, Abdalla S, Chen P, Liu Y, Bennett B, Khalil N, Sutherland D, Smith W, Horan G, Assaf M, Horowitz Z, Chopra R, Stevens RM, Palmisano M, Janssen-Heininger YM, and Schafer PH (2016) JNK inhibition reduces lung remodeling and pulmonary fibrotic systemic markers. Clin Transl Med 5, 36 [PubMed: 27590145]

47. Osto E, Matter CM, Kouroedov A, Malinski T, Bachschmid M, Camici GG, Kilic U, Stallmach T, Boren J, Iliceto S, Luscher TF, and Cosentino F (2008) c-Jun N-terminal kinase 2 deficiency protects against hypercholesterolemia-induced endothelial dysfunction and oxidative stress. Circulation 118, 2073–2080 [PubMed: 18955669]

48. Ricci R, Sumara G, Sumara I, Rozenberg I, Kurrer M, Akhmedov A, Hersberger M, Eriksson U, Eberli FR, Becher B, Boren J, Chen M, Cybulsky MI, Moore KJ, Freeman MW, Wagner EF, Matter CM, and Luscher TF (2004) Requirement of JNK2 for scavenger receptor A-mediated foam cell formation in atherogenesis. Science 306, 1558–1561 [PubMed: 15567863]

49. Amini N, Boyle JJ, Moers B, Warboys CM, Malik TH, Zakkar M, Francis SE, Mason JC, Haskard DO, and Evans PC (2014) Requirement of JNK1 for endothelial cell injury in atherogenesis. Atherosclerosis 235, 613–618 [PubMed: 24956536]

50. Liang Q, Bueno OF, Wilkins BJ, Kuan CY, Xia Y, and Molkentin JD (2003) c-Jun N-terminal kinases (JNK) antagonize cardiac growth through cross-talk with calcineurin-NFAT signaling. EMBO J 22, 5079–5089 [PubMed: 14517246]

51. Drake MJ, Williams J, and Bijos DA (2014) Voiding dysfunction due to detrusor underactivity: an overview. Nat Rev Urol 11, 454–464 [PubMed: 25002201]

52. Schmid E, Osborn M, Rungger-Brandle E, Gabbiani G, Weber K, and Franke WW (1982) Distribution of vimentin and desmin filaments in smooth muscle tissue of mammalian and avian aorta. Exp Cell Res 137, 329–340 [PubMed: 7035200]

53. Gabbiani G, Schmid E, Winter S, Chaponnier C, de Ckhastonay C, Vandekerckhove J, Weber K, and Franke WW (1981) Vascular smooth muscle cells differ from other smooth muscle cells: predominance of vimentin filaments and a specific alpha-type actin. Proc Natl Acad Sci U S A 78, 298–302 [PubMed: 7017714]

54. Osborn M, Caselitz J, and Weber K (1981) Heterogeneity of intermediate filament expression in vascular smooth muscle: a gradient in desmin positive cells from the rat aortic arch to the level of the arteria iliaca communis. Differentiation 20, 196–202 [PubMed: 7040147]

55. Despa S, Margulies KB, Chen L, Knowlton AA, Havel PJ, Taegtmeyer H, Bers DM, and Despa F (2012) Hyperamylinemia contributes to cardiac dysfunction in obesity and diabetes: a study in humans and rats. Circ Res 110, 598–608 [PubMed: 22275486]
56. Gianni D, Li A, Tesco G, McKay KM, Moore J, Raygor K, Rota M, Gwathmey JK, Dec GW, Aretz T, Leri A, Semigran MJ, Anversa P, Macgillivray TE, Tanzi RE, and del Monte F (2010) Protein aggregates and novel presenilin gene variants in idiopathic dilated cardiomyopathy. Circulation 121, 1216–1226 [PubMed: 20194882]
57. Nagai R, Kuro-o M, Babij P, and Periasamy M (1989) Identification of two types of smooth muscle myosin heavy chain isoforms by cDNA cloning and immunoblot analysis. J Biol Chem 264, 9734–9737 [PubMed: 2722872]
58. Owens GK (1995) Regulation of differentiation of vascular smooth muscle cells. Physiol Rev 75, 487–517 [PubMed: 7624392]
59. Woodcock-Mitchell J, Mitchell JJ, Low RB, Kieny M, Sengel P, Rubbia L, Skalli O, Jackson B, and Gabbiani G (1988) Alpha-smooth muscle actin is transiently expressed in embryonic rat cardiac and skeletal muscles. Differentiation 39, 161–166 [PubMed: 2468547]
60. Darby I, Skalli O, and Gabbiani G (1990) Alpha-smooth muscle actin is transiently expressed by myofibroblasts during experimental wound healing. Lab Invest 63, 21–29 [PubMed: 2197503]
61. Solway J, Seltzer J, Samaha FF, Kim S, Alger LE, Niu Q, Morrisey EE, Ip HS, and Parmacek MS (1995) Structure and expression of a smooth muscle cell-specific gene, SM22 alpha. J Biol Chem 270, 13460–13469
62. Zhang JC, Kim S, Helmke BP, Yu WW, Du KL, Lu MM, Strobeck M, Yu Q, and Parmacek MS (2001) Analysis of SM22alpha-deficient mice reveals unanticipated insights into smooth muscle cell differentiation and function. Mol Cell Biol 21, 1336–1344 [PubMed: 11158319]
63. Kim HD (1996) Expression of intermediate filament desmin and vimentin in the human fetal heart. Anat Rec 246, 271–278 [PubMed: 8888968]
64. Fuchs E, and Weber K (1994) Intermediate filaments: structure, dynamics, function, and disease. Annu Rev Biochem 63, 345–382 [PubMed: 7979242]
65. Council L, and Hameed O (2009) Differential expression of immunohistochemical markers in bladder smooth muscle and myofibroblasts, and the potential utility of desmin, smoothelin, and vimentin in staging of bladder carcinoma. Mod Pathol 22, 639–650 [PubMed: 19252475]
66. Capetanaki Y, Smith S, and Heath JP (1989) Overexpression of the vimentin gene in transgenic mice inhibits normal lens cell differentiation. J Cell Biol 109, 1653–1664 [PubMed: 2793935]
67. Osman NI, and Chapple CR (2018) Are There Pharmacotherapeutic Options for Underactive Bladder? Eur Urol Focus 4, 6–7 [PubMed: 29776685]

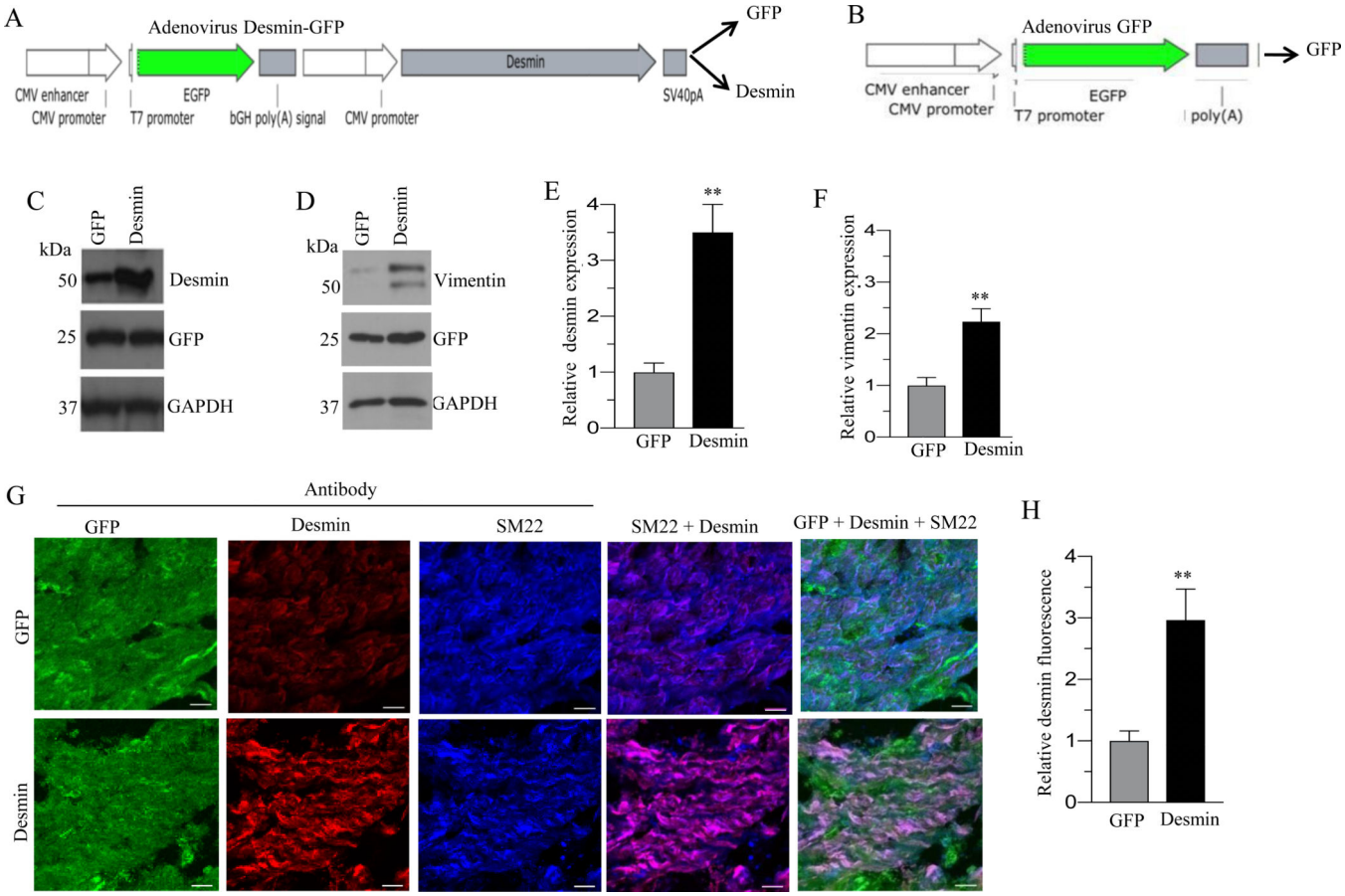

Figure 1. Adenovirus mediated overexpression of desmin in murine BSM strips.

A: Schematic depiction of desmin-GFP bicistronic adenoviral vector construct. B: Schematic depiction of GFP adenoviral vector construct C-D: Murine BSM strips devoid of urothelium and submucosa were transduced with an adenovirus encoding GFP and desmin for 48 h and the expression levels of desmin, vimentin and GFP proteins were determined by immunoblot analysis. GAPDH was used as a loading control. E-F: Quantification of immunoblot data. G: Sections prepared from murine BSM strips overexpressing desmin and GFP proteins were stained with anti-desmin, anti-SM22 and Alexa Fluor 488 labelled GFP antibody, followed by Cy3 and Cy5 conjugated secondary antibodies. Representative confocal images are shown. Scale bars = 10 μm. H: Quantification of confocal images data. Data are expressed as means ± SD (E, F & H), n = 5 mice in each group (E, F & H). **, $P < 0.01$ versus GFP expressing murine BSM strips.

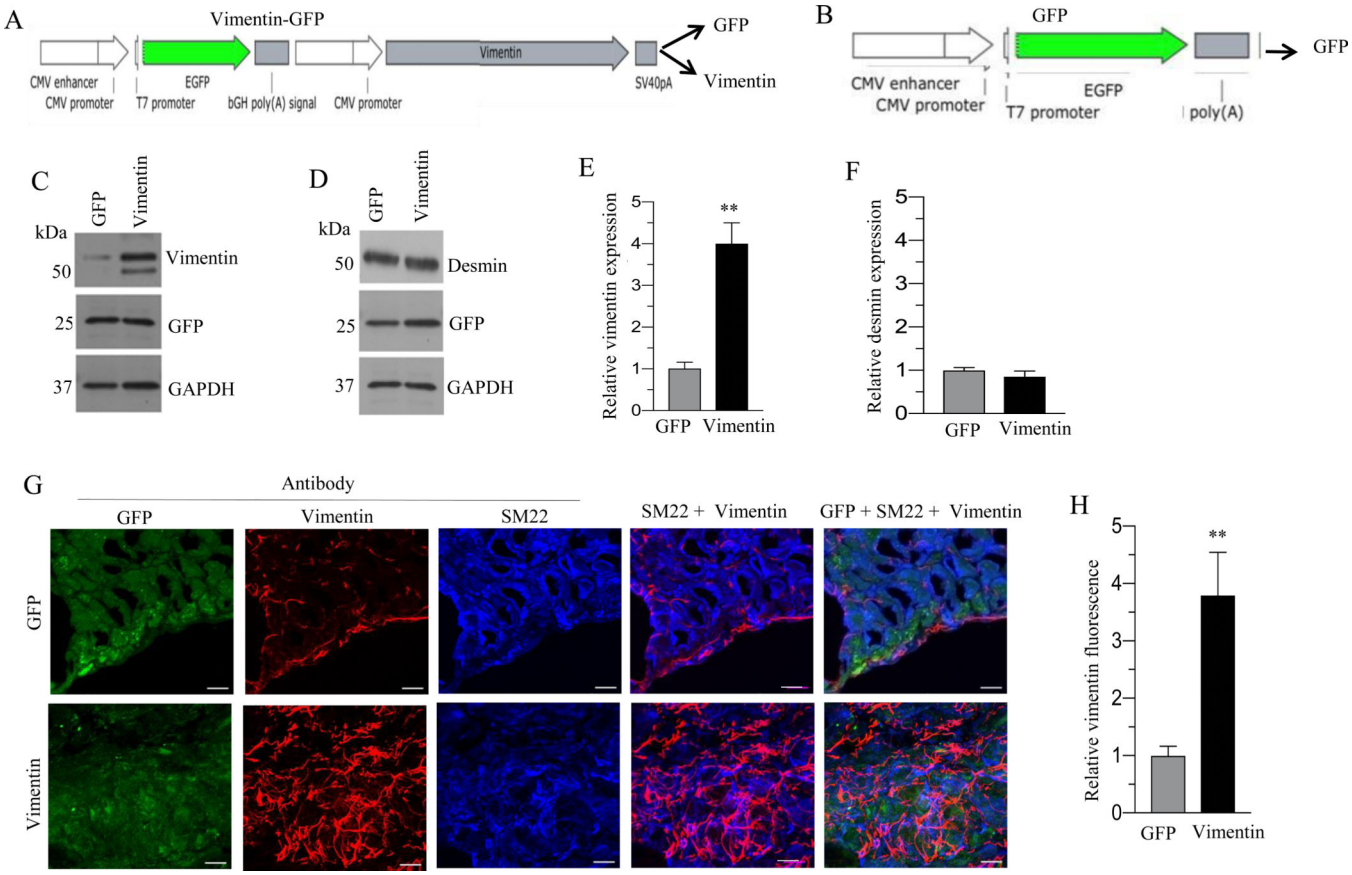

Figure 2. Adenovirus mediated overexpression of vimentin in murine BSM strips.

A: Schematic depiction of vimentin-GFP bicistronic adenoviral vector construct. B: Schematic depiction of GFP adenoviral vector construct. C-D: Murine BSM strips devoid of urothelium and submucosa were transduced with an adenovirus encoding GFP and vimentin for 48 h and the expression levels of vimentin, desmin and GFP proteins were determined by immunoblot analysis. GAPDH was used as a loading control. E-F: Quantification of immunoblot data. G: Sections prepared from murine BSM strips overexpressing vimentin and GFP proteins were stained with anti-vimentin, anti-SM22 and Alexa Fluor 488 labelled GFP antibody, followed by Cy3 and Cy5 conjugated secondary antibodies. Representative confocal images are shown. Scale bars = 10 μm. H: Quantification of confocal images data. Data are expressed as means ± SD (E, F & H), n = 5 mice in each group (E, F & H). **, $P < 0.01$ versus GFP expressing murine BSM strips.

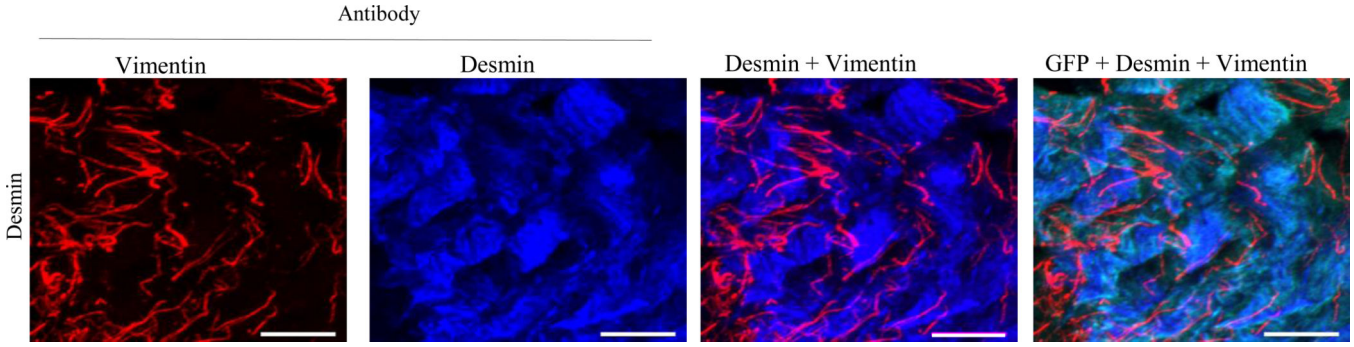

Figure 3. Co-localization of desmin and vimentin in murine BSM strips overexpressing desmin.
Sections prepared from murine BSM strips overexpressing desmin were stained with anti-vimentin, anti-desmin and Alexa Fluor 488 labelled GFP antibody, followed by Cy3 and Cy5 conjugated secondary antibodies. Representative confocal images are shown. Scale bars = 10 μm.

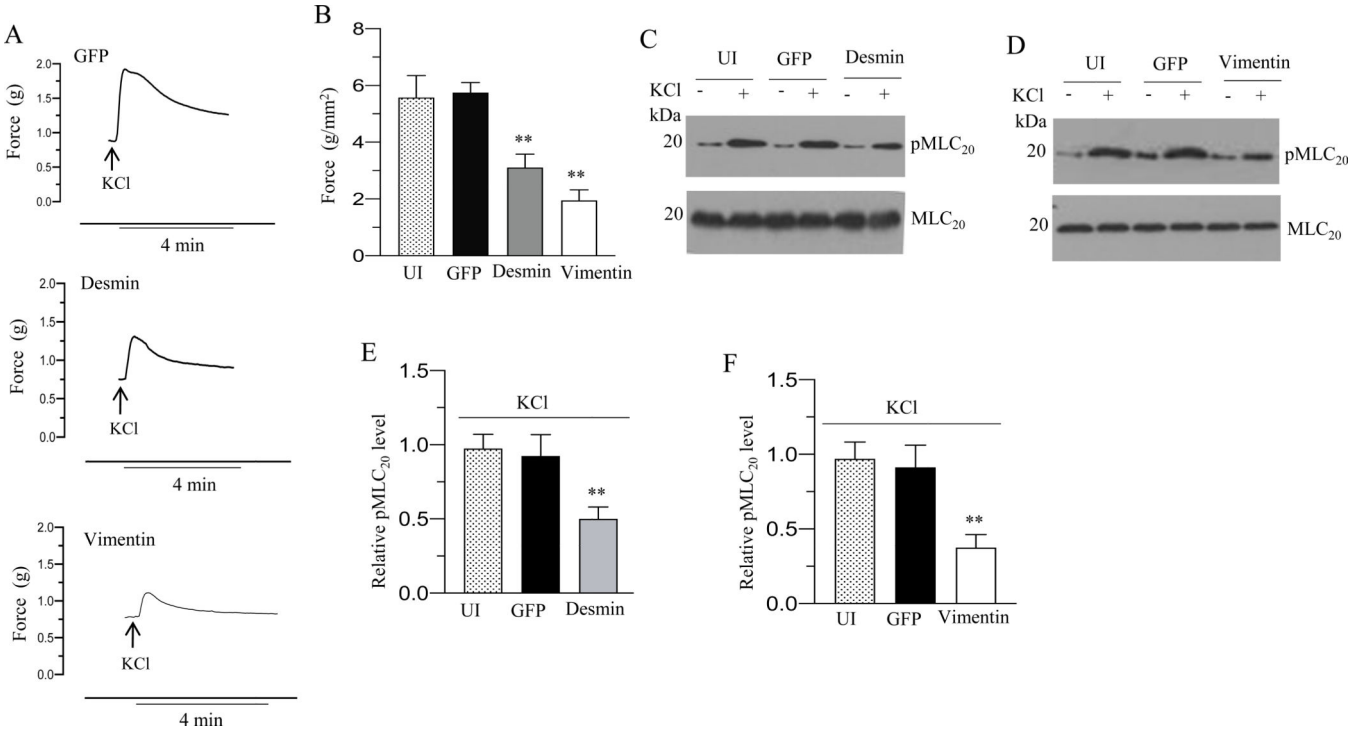

Figure 4. Desmin and vimentin overexpression reduces murine BSM contraction and MLC_{20} phosphorylation in response to membrane depolarization.

Murine BSM strips devoid of urothelium and submucosa were transduced with an adenovirus encoding GFP, desmin and vimentin for 48 h and the contractile responses and MLC_{20} phosphorylation of muscle strips were determined in response to membrane depolarization. A: Representative traces of contraction produced by murine BSM strips overexpressing GFP, desmin, and vimentin in response to KCl stimulation (120 mM). Arrows indicate the addition of high K^+ Tyrode buffer to the organ bath. B: Quantitation of contractile response in response to KCl stimulation. The data is presented as grams per cross sectional area (g/mm^2) for uninfected murine BSM strips and GFP, desmin and vimentin overexpressing murine BSM strips. C-D: Immunoblot analysis of KCl-stimulated MLC_{20} phosphorylation in uninfected murine BSM strips and in murine BSM strips overexpressing GFP, desmin and vimentin. BSM strips were contracted for 20 seconds with KCl (120 mM) and rapidly frozen at 0 sec (resting) and 20 sec of contraction and then the muscle strips were processed for MLC_{20} phosphorylation. E-F: Quantification of immunoblots (C & D). Data are expressed as means ± standard error mean (SEM), n = 7 mice in each group. **, $P \leq 0.05$ versus GFP expressing murine BSM strips in (B). $P \leq 0.01$ versus GFP expressing murine BSM strips in (E-F).

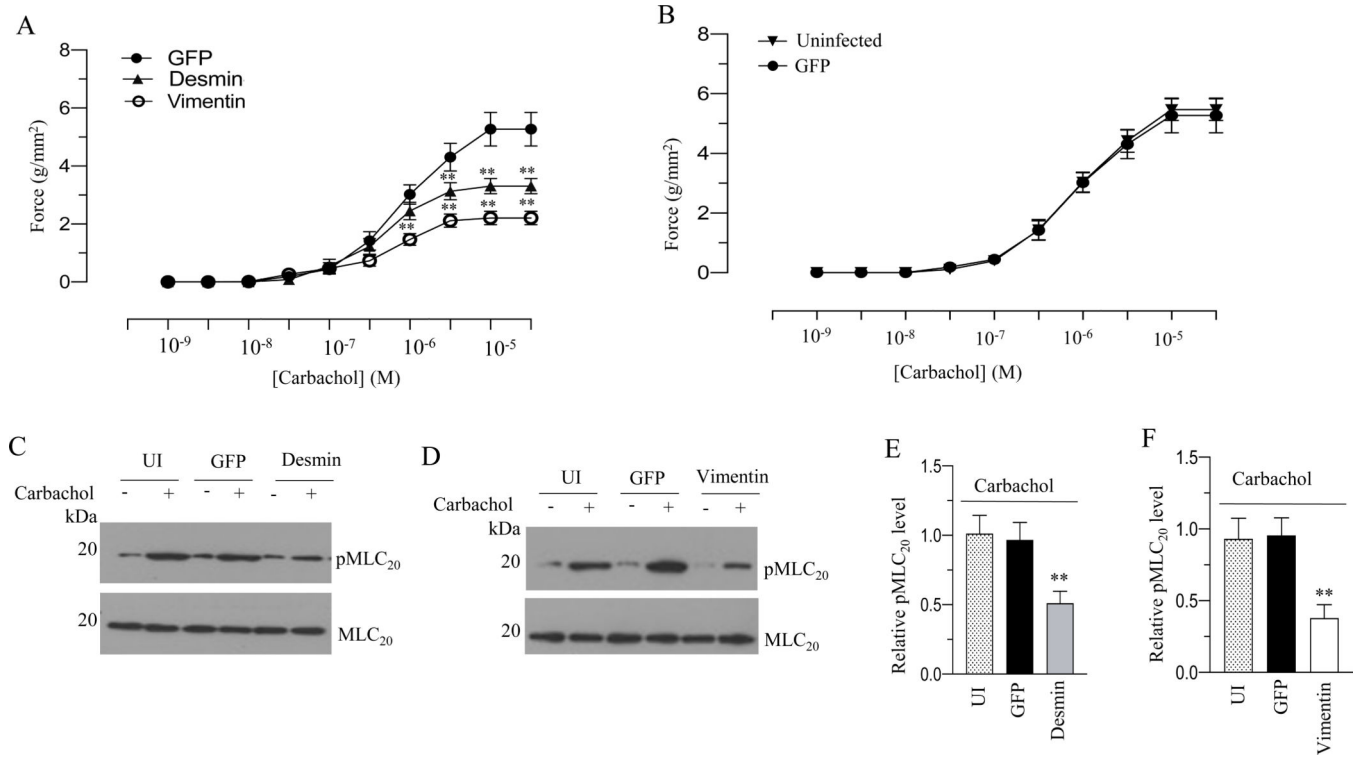

Figure 5. Desmin and vimentin overexpression reduces murine BSM contraction and MLC_{20} phosphorylation in response to cholinergic agonist.

Murine BSM strips devoid of urothelium and submucosa were transduced with an adenovirus encoding GFP, desmin and vimentin for 48 h and the contractile responses and MLC_{20} phosphorylation of muscle strips were determined in response to cholinergic agonist. A: Concentration dependent contractile response (cumulative carbachol concentration 10^{-9} to 3×10^{-5} M) by murine BSM strips overexpressing GFP, desmin, and vimentin. Data is presented as grams per cross sectional area (g/mm^2). B: Concentration dependent contractile response (cumulative carbachol concentration 10^{-9} to 3×10^{-5} M) by murine BSM strips overexpressing GFP and uninfected murine BSM strips (without GFP expression). The data is presented as grams per cross sectional area (g/mm^2). C-D: Immunoblot analysis of carbachol-stimulated MLC_{20} phosphorylation in uninfected murine BSM strips and in murine BSM strips overexpressing GFP, desmin or vimentin. BSM strips were contracted for 30 seconds with carbachol (10 μM) and rapidly frozen at 0 sec (resting) and 30 sec of contraction and then the muscle strips were processed for MLC_{20} phosphorylation. E-F: Quantification of immunoblots (C & D). Data are expressed as means ± standard error mean (SEM), n = 7 mice in each group. **, $P \leq 0.05$ versus GFP expressing murine BSM strips in (A). **, $P \leq 0.01$ versus murine BSM strips expressing GFP in (E-F).

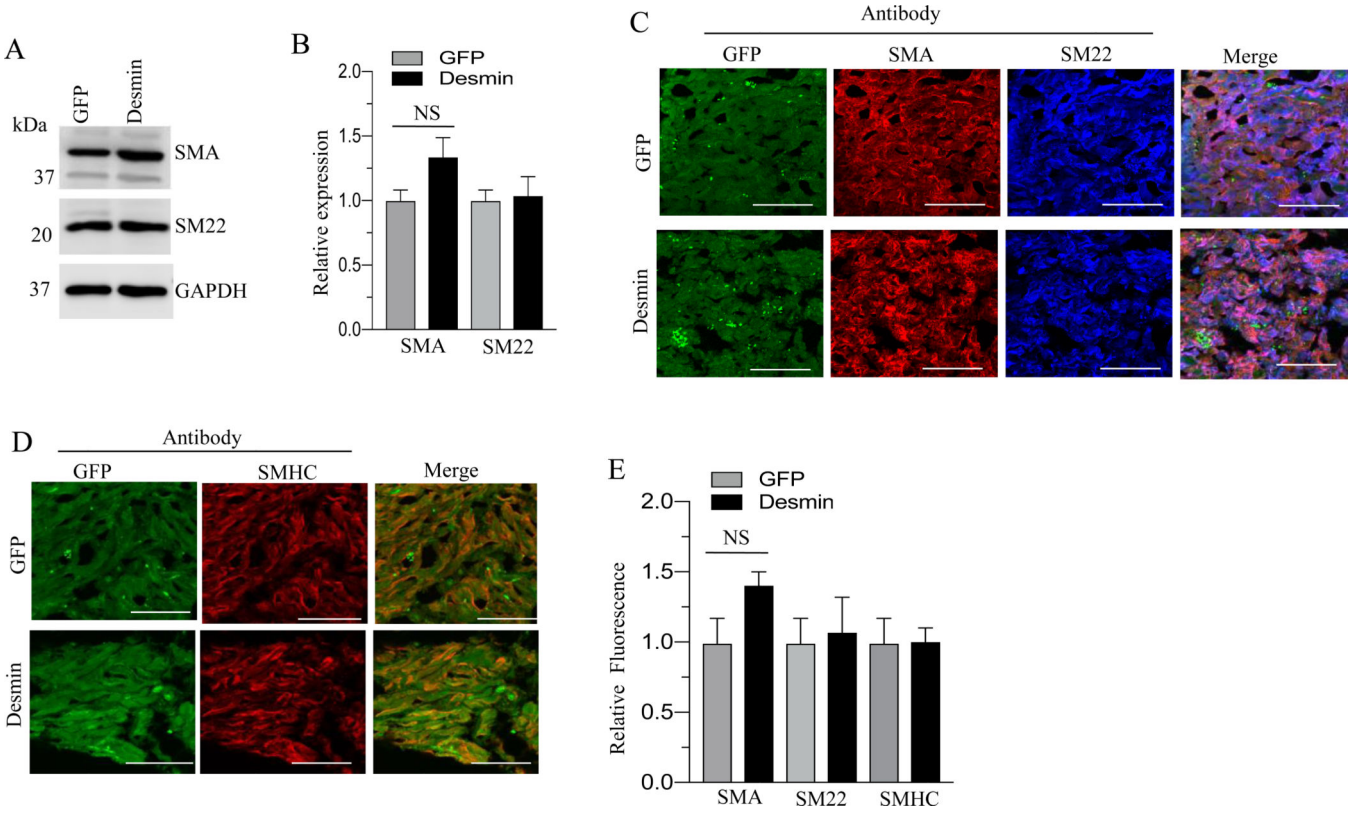

Figure 6. Effect of desmin overexpression on smooth muscle marker proteins expression in murine BSM.

A: Murine BSM strips devoid of urothelium and submucosa were transduced with an adenovirus encoding GFP, and desmin for 48 h and the expression levels of SMA, and SM22 were determined by immunoblot analysis. GAPDH was used as a loading control. B: Quantification of immunoblot data. C-D: Sections prepared from murine BSM strips overexpressing desmin and GFP proteins were stained with anti-SMA, or anti-SM22. or anti-SMHC or Alexa Fluor 488 labelled GFP antibody, followed by Cy3 and Cy5 conjugated secondary antibodies. Representative confocal images are shown in C and D: Scale bars = 50 μm. E: Quantification of confocal images data. Data are expressed as means ± SD, n = 5 mice in each group. NS indicates non significant.

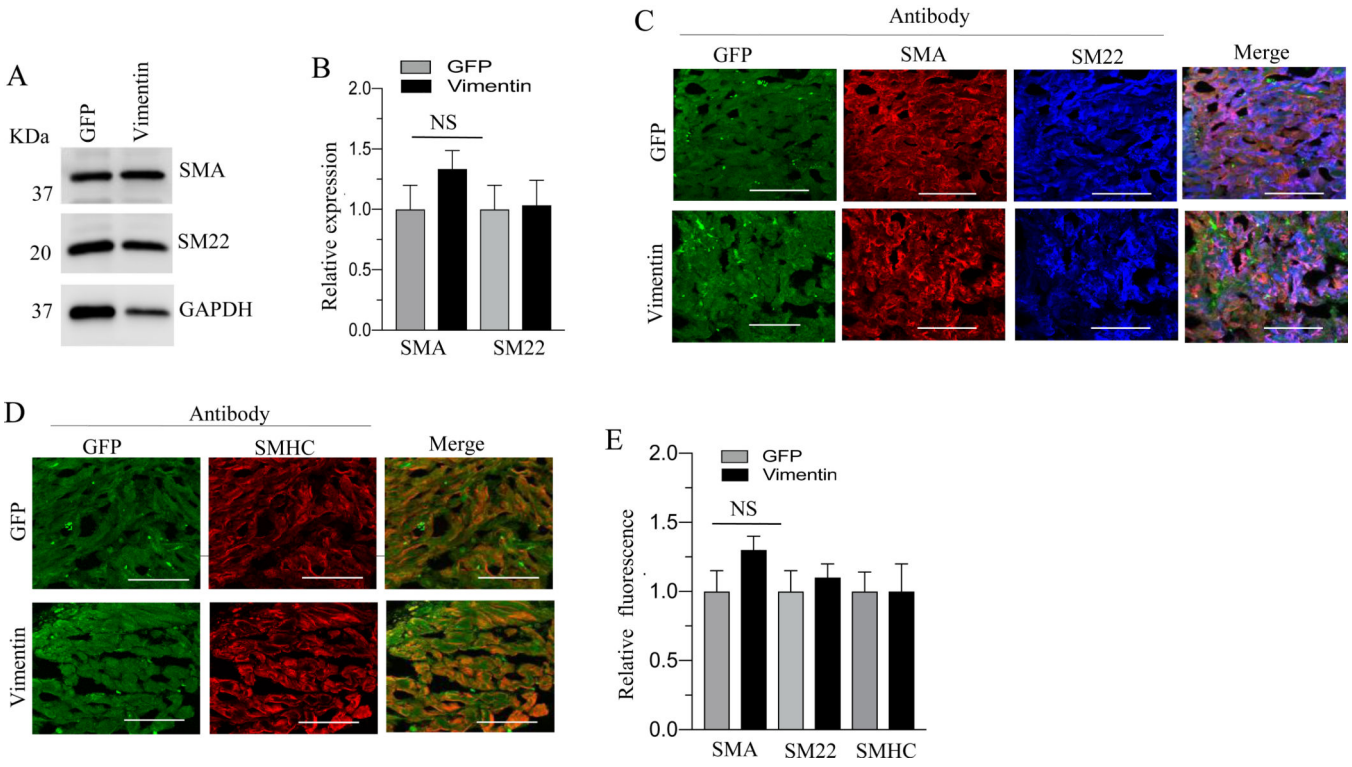

Figure 7. Effect of vimentin overexpression on smooth muscle marker proteins expression in murine BSM.

A: Murine BSM strips devoid of urothelium and submucosa were transduced with an adenovirus encoding GFP, and vimentin for 48 h and the expression levels of SMA, and SM22 were determined by immunoblot analysis. GAPDH was used as a loading control. B: Quantification of immunoblot data. C-D: Sections prepared from murine BSM strips overexpressing vimentin and GFP proteins were stained with anti-SMA, or anti- SM22, or anti-SMHC or Alexa Fluor 488 labelled GFP antibody, followed by Cy3 and Cy5 conjugated secondary antibodies. Representative confocal images are shown in C and D: Scale bars = 50 μm. E: Quantification of confocal images data. Data are expressed as means ± SD, n = 5 mice in each group. NS indicates non significant.

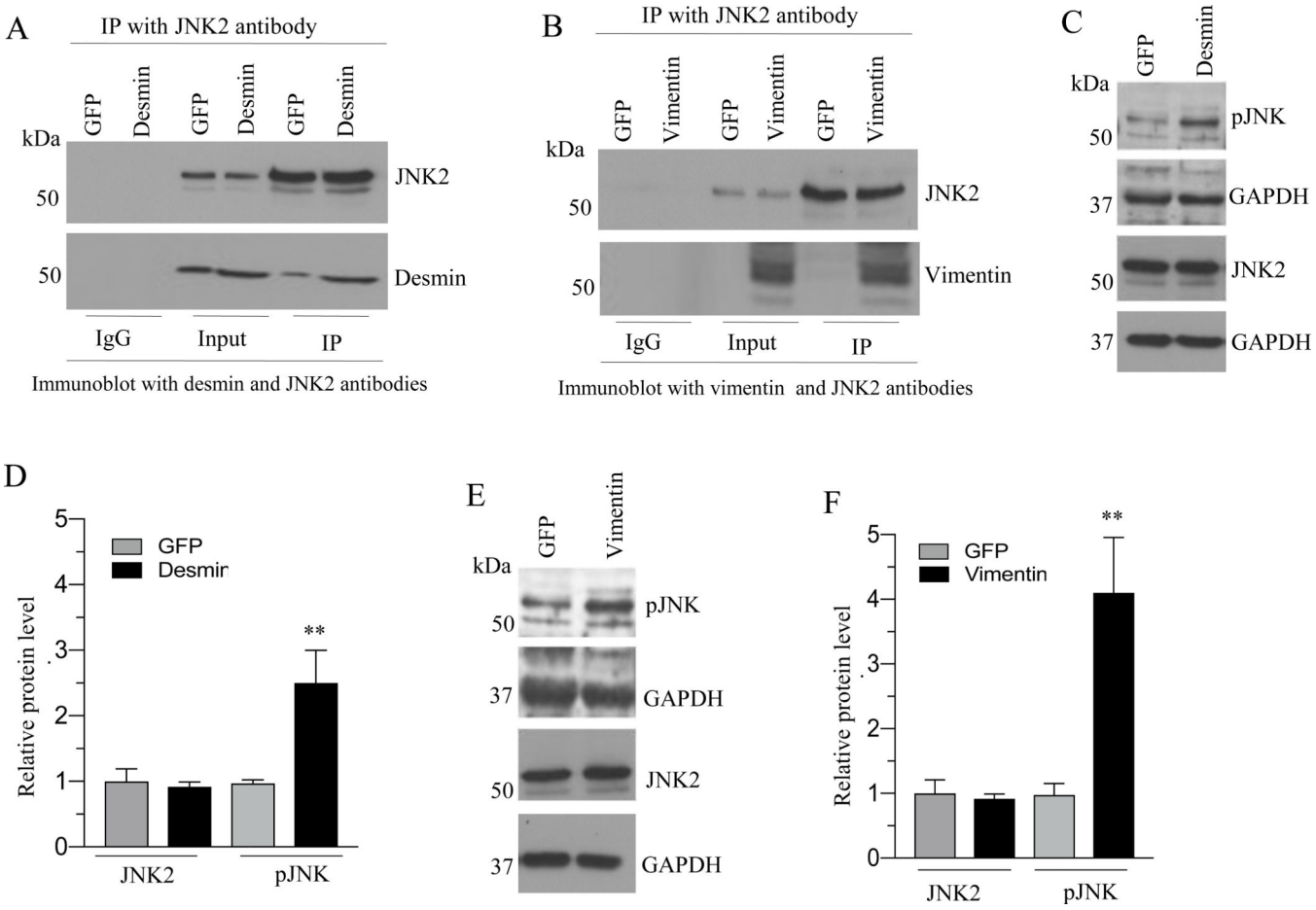

Figure 8. Desmin and vimentin interact with JNK2 and enhance the phospho JNK level following the IF protein overexpression in murine BSM.

A-B: Murine BSM strips devoid of urothelium and submucosa were transduced with an adenovirus encoding GFP, desmin and vimentin for 48 h and the total proteins from GFP, desmin and vimentin overexpressing murine BSM strips were immunoprecipitated with JNK2 antibody. The resulting immunoprecipitate was separated on a SDS-PAGE and subsequently probed with either anti-desmin and anti-JNK2 antibodies (A) or anti-vimentin and anti JNK2 antibodies (B). The input served as a loading control in both (A) and (B). C-F: Increased levels of phospho JNK following desmin and vimentin overexpression. Total proteins extracted from GFP, desmin and vimentin overexpressing murine BSM strips were subjected to immunoblot analysis using phosphorylated JNK and total JNK2 antibodies. GAPDH was used as a loading control. D & F: Quantification of immunoblots (C & E). Data are expressed as means ± SD, n = 5 mice in each group. **, $P < 0.01$ versus GFP expressing murine BSM strips.

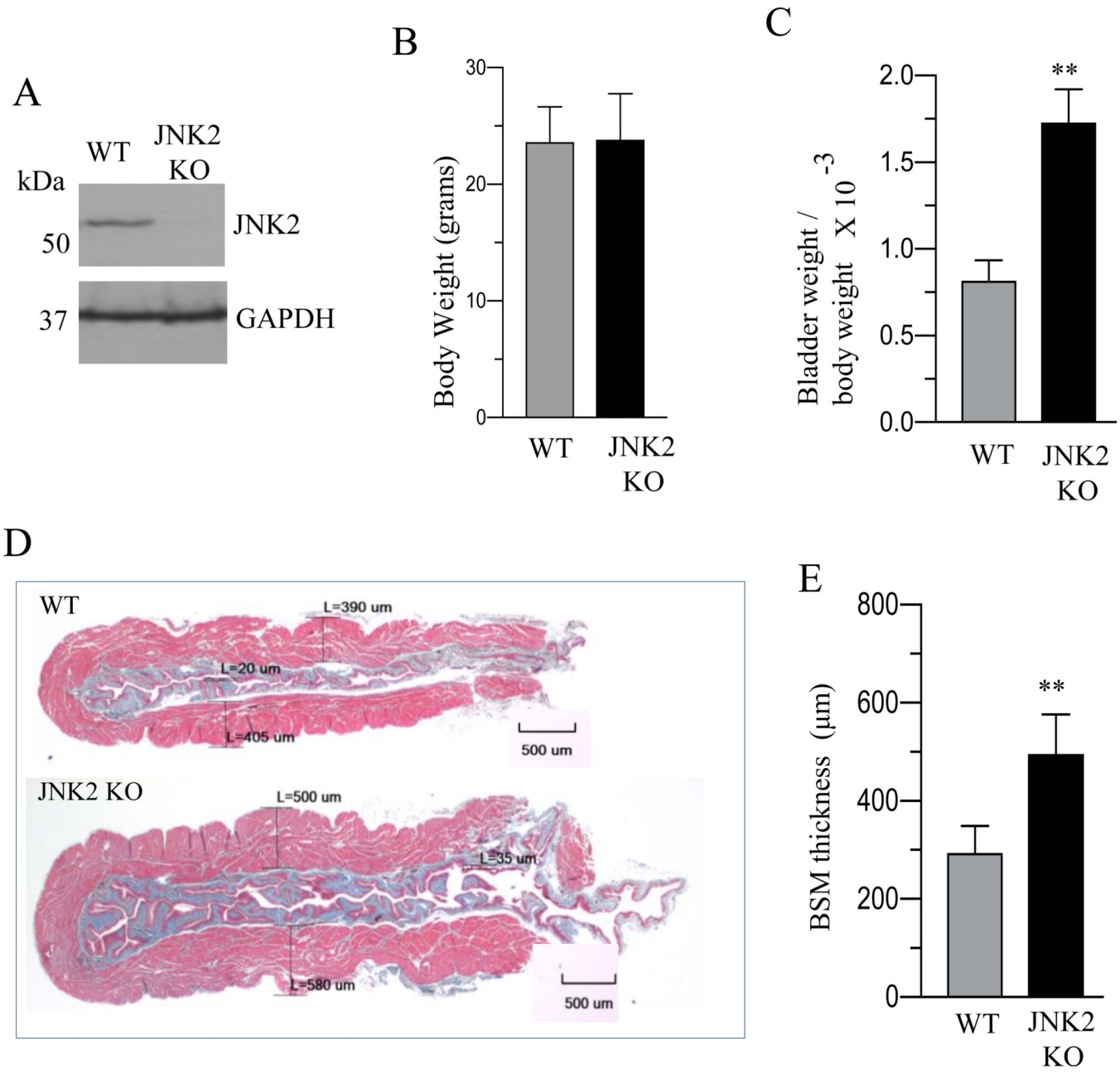

Figure 9. Increased bladder muscle mass in JNK2 KO mice.

A: Total proteins of BSM strips from WT and JNK2 KO mice were subjected to immunoblot analysis and the expression level of JNK2 was determined. Representative immunoblot showing the expression level of JNK2 in JNK2 KO mice compared with WT mice. GAPDH was used as a loading control. B-C: Body weights, and bladder weight to body weight ratio of WT and JNK2 KO mice are shown. D: Masson trichrome staining of bladder cross sections of WT and JNK2 KO mice is shown. The red staining in each image is smooth muscle bundles. The blue staining in each image is collagen fibers. Scale bars = 500 µm E: Quantification of trichrome image. Data are expressed as means ± SD (B, C and E), n = 10

mice in each group (B and C); n = 4 mice in each group (A & E). **, P < 0.01 versus WT mice.

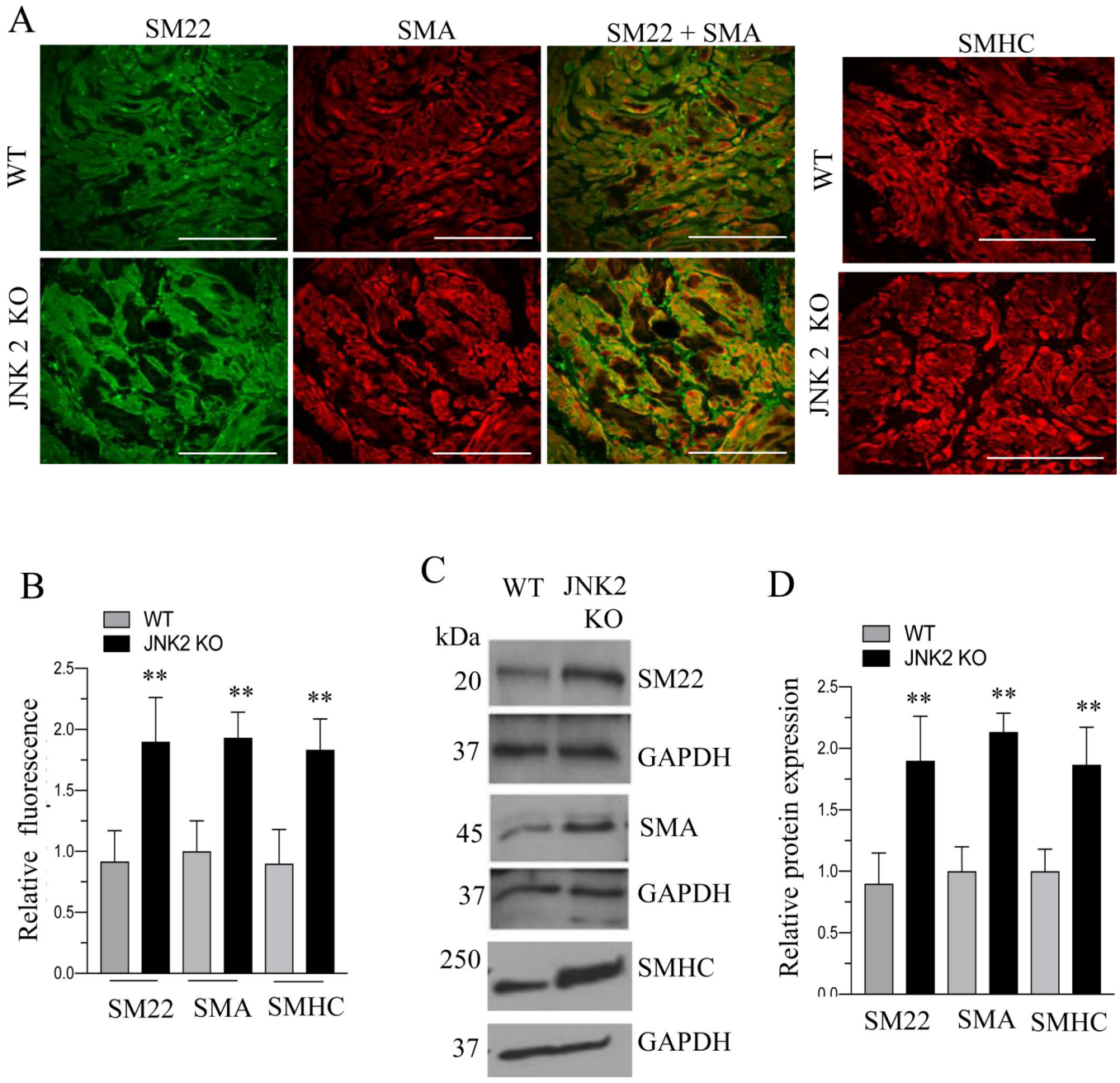

Figure 10. JNK2 deficiency enhances contractile proteins expression.

A: Immunofluorescence analysis of smooth muscle marker proteins expression in WT and JNK2 KO mice. Bladder sections prepared from WT and JNK2 KO mice were stained with anti-SMA or anti-SM22 or SMHC antibody followed by Cy3- and Alexa Fluor 488 conjugated secondary antibodies. Representative confocal images are shown. Scale bars = 50 μm. B: Quantification of confocal images. Data are expressed as means ± SEM. n = 5 mice in each group. **, $P < 0.01$ versus WT mice. C: Total proteins of BSM strips from WT and JNK2 KO mice were subjected to immunoblot analysis and the expression levels of smooth

muscle marker proteins were determined. Representative immunoblot is shown. GAPDH was used as a loading control. D: Quantification of immunoblot.

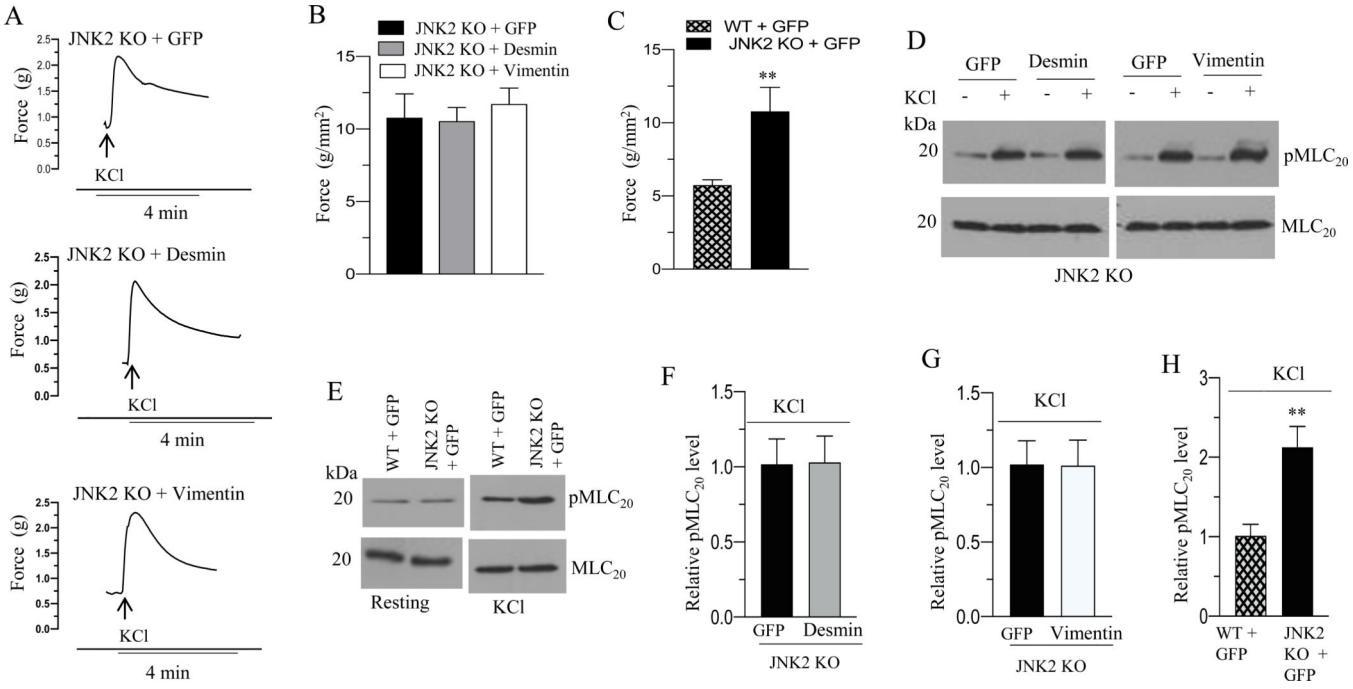

Figure 11. Increased expression of desmin and vimentin does not alter BSM contraction and MLC_{20} phosphorylation in response to KCl in JNK2 KO mice.

A-E: Murine BSM strips devoid of urothelium and submucosa from JNK2 KO mice were transduced with an adenovirus encoding GFP or desmin or vimentin for 48 h and the contractile properties and MLC_{20} phosphorylation of these strips were determined. A: Representative traces of contraction produced by BSM strips from JNK2 KO mice overexpressing GFP, desmin, or vimentin in response to KCl stimulation (120 mM). Arrows indicate the addition of high K^+ Tyrode buffer to the organ bath. B: Quantitation of contractile response in response to KCl stimulation (120 mM) by JNK2 KO murine BSM strips overexpressing GFP, desmin or vimentin. The data is presented as grams per cross sectional area (g/mm^2). C: Contractile response in response to KCl stimulation (120 mM) by WT and JNK2 KO murine BSM strips expressing GFP. The data is presented as grams per cross sectional area (g/mm^2). D-E: Immunoblot analysis of KCl- stimulated MLC_{20} phosphorylation in murine BSM strips from WT and JNK2 KO mice overexpressing GFP, desmin or vimentin. BSM strips were contracted for 20 seconds with KCl (120 mM) and rapidly frozen at 0 sec (resting) and 20 sec of contraction and then processed the muscle strips for MLC_{20} phosphorylation. F-H: Quantification of immunoblots (D & E). Data are expressed as means ± standard error mean (SEM), n = 7 mice in each group. **, $P \leq 0.05$ versus WT murine BSM strips expressing GFP in (C). **, $P \leq 0.01$ versus WT murine BSM strips expressing GFP in (H).

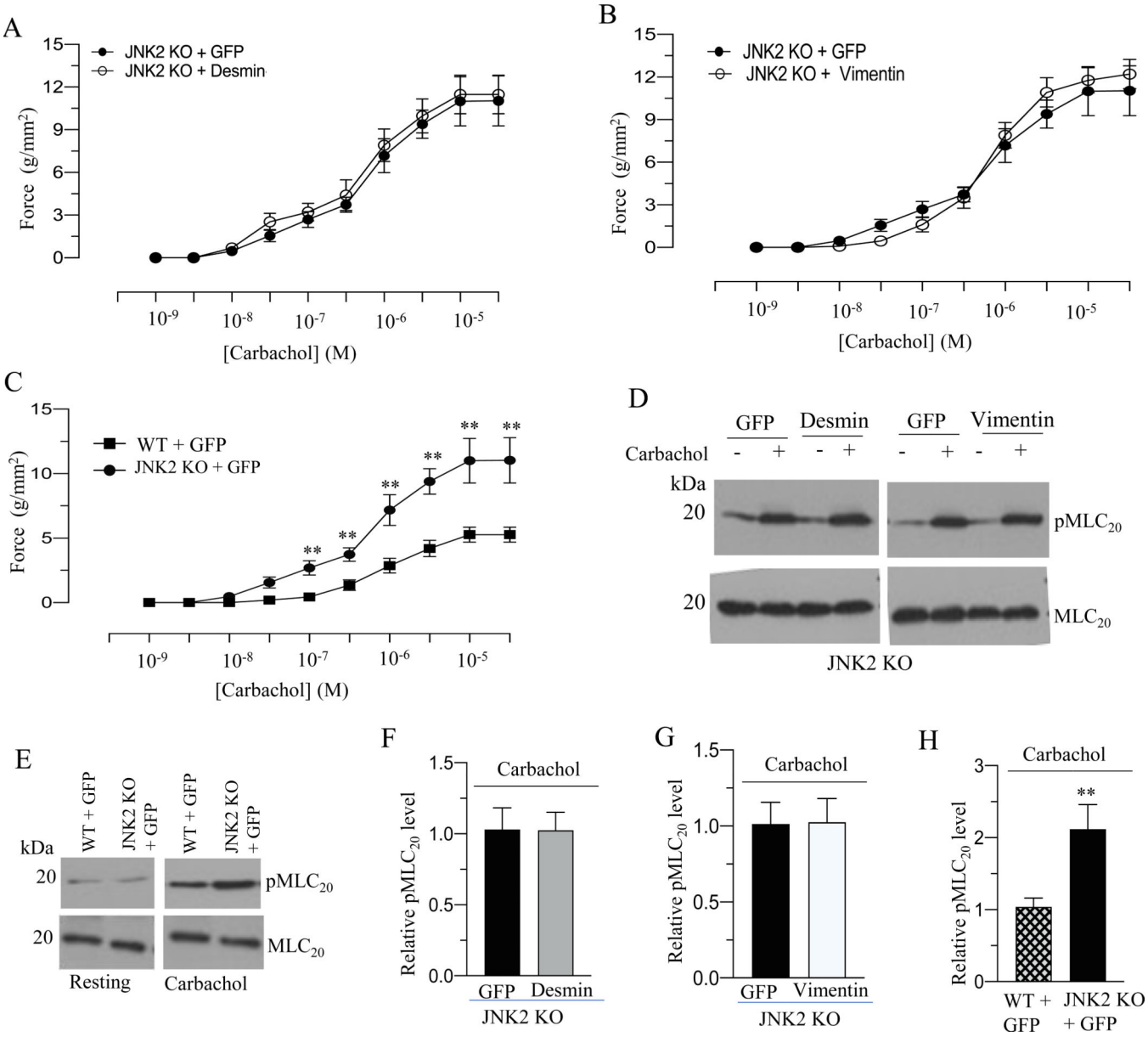

Figure 12. Increased expression of desmin and vimentin does not alter BSM contraction and MLC_{20} phosphorylation in response to carbachol in JNK2 KO mice.

A-E: Murine BSM strips devoid of urothelium and submucosa from JNK2 KO mice were transduced with an adenovirus encoding GFP or desmin or vimentin- for 48 h and the contractile properties and MLC_{20} phosphorylation of these strips were determined in response to carbachol. A-B: Concentration dependent contractile response (cumulative carbachol concentration, 10^{-9} to 3×10^{-5} M) by JNK2 KO murine BSM strips overexpressing GFP, desmin, or vimentin. The data is presented as grams per cross sectional area (g/mm^2). C: Concentration dependent contractile response (cumulative carbachol concentration, 10^{-9} to 3×10^{-5} M) by WT and JNK2 KO murine BSM strips expressing GFP. The data is presented as grams per cross sectional area (g/mm^2). D-E: Immunoblot analysis of carbachol-stimulated MLC_{20} phosphorylation in murine BSM strips from JNK2

KO and WT mice overexpressing GFP, desmin or vimentin. BSM strips were contracted for 30 seconds with carbachol (10 μM) and rapidly frozen at 0 sec (resting) and 30 sec of contraction and then processed the muscle strips for MLC_{20} phosphorylation. F-H: Quantification of immunoblots (D & E). Data are expressed as means ± standard error mean (SEM), n = 7 mice in each group. **, $P \leq 0.05$ versus WT murine BSM strips expressing GFP in (C). **, $P \leq 0.01$ versus WT murine BSM strips expressing GFP in (H).

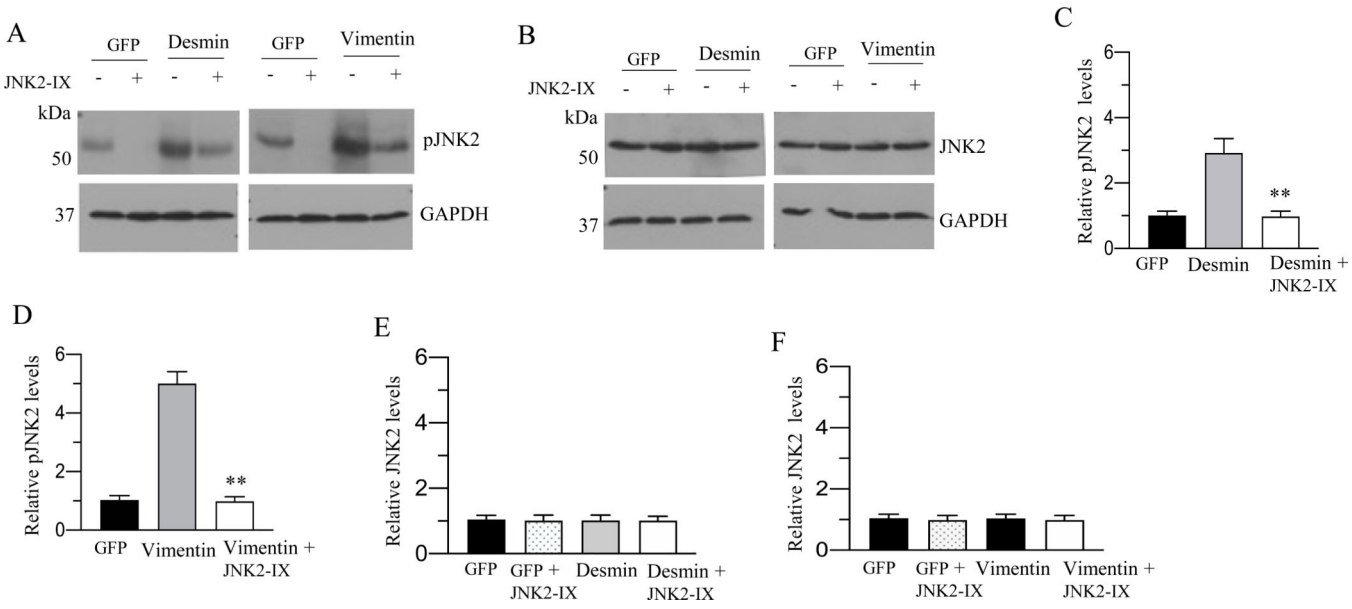

Figure 13. JNK2 inhibitor reduces phospho JNK2 level following desmin and vimentin protein overexpression.

A-B: Murine BSM strips devoid of urothelium and submucosa were transduced with an adenovirus encoding GFP, desmin or vimentin for 48 h in the presence or absence of a JNK2 specific inhibitor, JNK2-IX (100 nM). Total proteins extracted from murine BSM strips overexpressing GFP, desmin or vimentin were subjected to immunoblot analysis using phosphorylated JNK and JNK2 antibodies. GAPDH was used as a loading control. C-F: Quantification of immunoblots (A & B). Data are expressed as means ± SD, n = 7 mice in each group. **, $P < 0.01$ versus murine BSM strips overexpressing desmin in (C). **, $P < 0.01$ versus murine BSM strips overexpressing vimentin in (D).

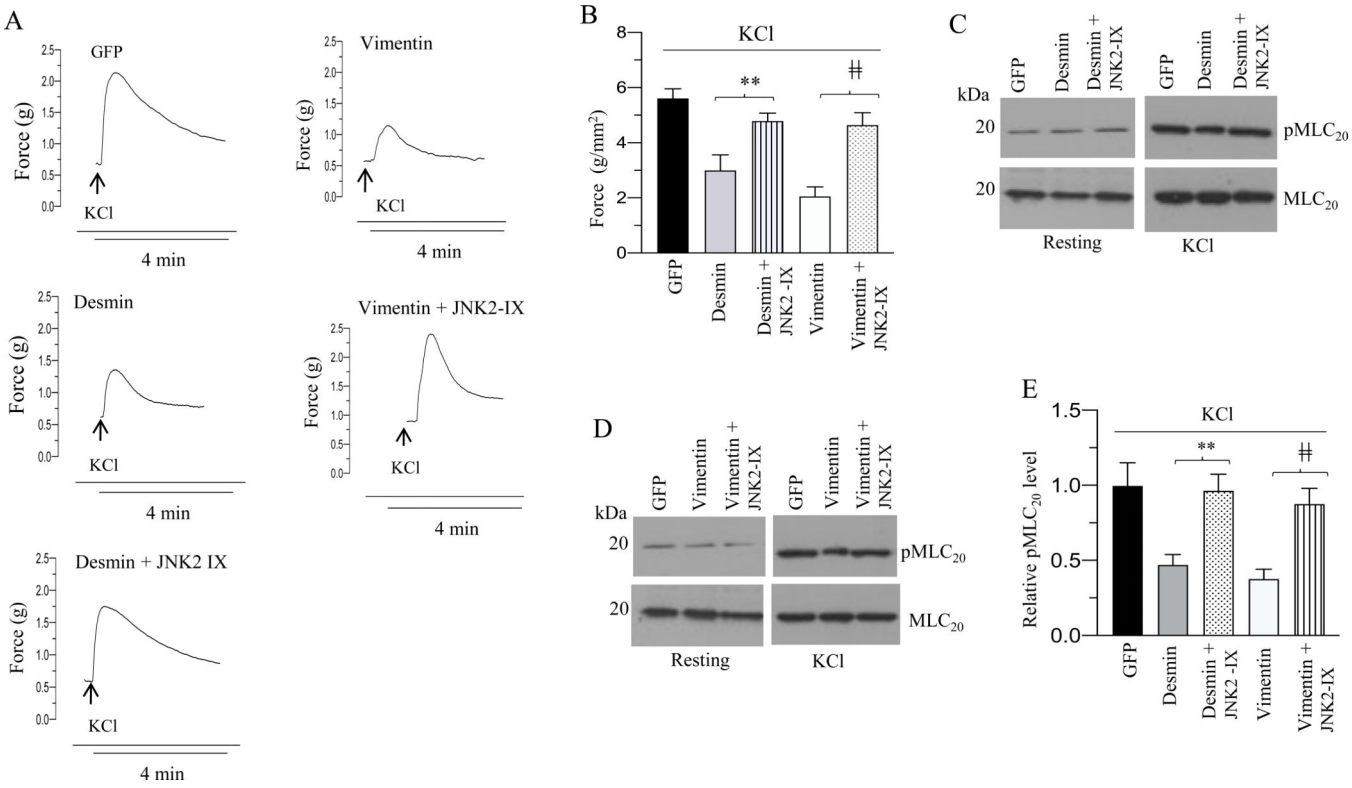

Figure 14. Pharmacological inhibition of JNK2 activity rescues the KCl-induced decreased contractile responses as well as the decrease in MLC_{20} phosphorylation observed with desmin or vimentin overexpression.

A-E: Murine BSM strips devoid of urothelium and submucosa were transduced with an adenovirus encoding GFP, desmin and vimentin for 48 h. In some cases, strips were treated with JNK2 specific inhibitor, JNK2-IX (100 nM) for 48 h. A: Representative traces of contraction produced by BSM strips overexpressing GFP, desmin, and vimentin in the presence or absence of JNK2-IX in response to KCl stimulation (120 mM). Arrows indicate the addition of high K^+ Tyrode buffer to the organ bath. B: Quantitation of contractile response produced by BSM strips overexpressing GFP, desmin, and vimentin in the presence or absence of JNK2-IX in response to KCl stimulation. The data is presented as grams per cross sectional area (g/mm^2). C-D: Immunoblot analysis of MLC_{20} phosphorylation in murine BSM strips overexpressing GFP, desmin or vimentin in the presence or absence of JNK2-IX (100 nM) in response to KCl stimulation. BSM strips were contracted for 20 seconds with KCl (120 mM) in the presence or absence of JNK2-IX (100 nM) and rapidly frozen at 0 sec (resting) and 20 sec of contraction and then processed the muscle strips for MLC_{20} phosphorylation. E: Quantification of immunoblots (C & D). Data are expressed as means ± standard error mean (SEM), n = 8 mice in each group. **, $P \leq 0.05$ versus murine BSM strips overexpressing desmin in (B). ‡‡, $P \leq 0.05$ versus murine BSM strips overexpressing vimentin in (B). **, $P \leq 0.01$ versus murine BSM strips overexpressing desmin in (E). ‡‡, $P \leq 0.01$ versus murine BSM strips overexpressing vimentin in (E).

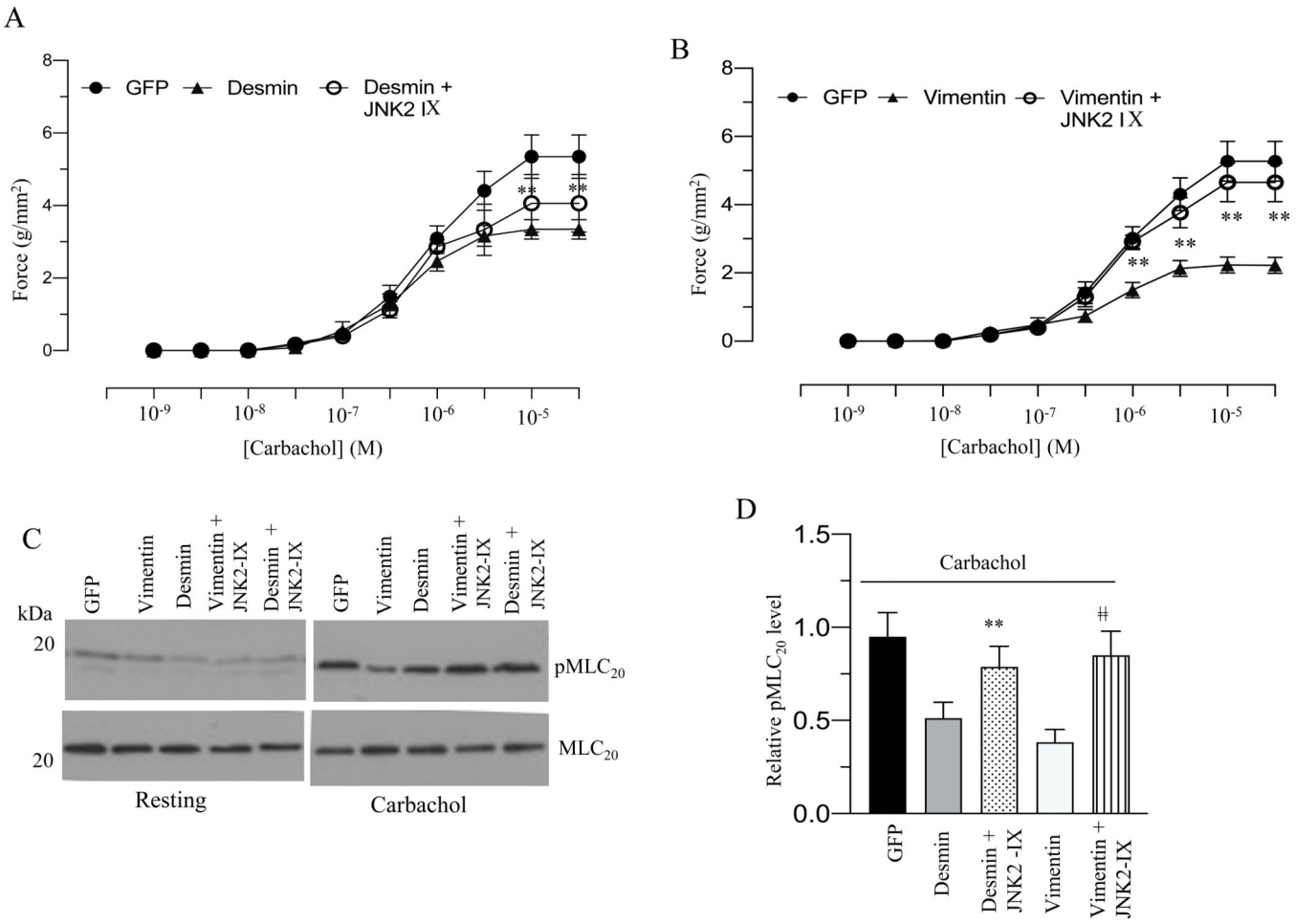

Figure 15. Pharmacological inhibition of JNK2 activity rescues the carbachol induced decreased contractile responses as well as the decrease in MLC_{20} phosphorylation observed with desmin or vimentin overexpression.

A-D: Murine BSM strips devoid of urothelium and submucosa were transduced with an adenovirus encoding GFP, desmin and vimentin for 48 h. In some cases, strips were treated with JNK2 specific inhibitor, JNK2-IX (100 nM) for 48 h. A-B: Concentration dependent contractile response (cumulative carbachol concentration, 10^{-9} to 3X 10^{-5} M) by murine BSM strips overexpressing GFP, desmin, and vimentin in the presence or absence of JNK2-IX. The data is presented as grams per cross sectional area (g/mm^2). C: Carbachol-stimulated MLC_{20} phosphorylation levels in murine BSM strips overexpressing GFP, desmin or vimentin in the presence or absence of JNK2-IX. BSM strips were contracted in the presence or absence of JNK2-IX (100 nM) for 30 seconds with carbachol (10 μM) and rapidly frozen at 0 sec (resting) and 30 sec of contraction and then processed the muscle strips for MLC_{20} phosphorylation. D: Quantification of immunoblot (C). Data are expressed as means ± standard error mean (SEM), n = 8 mice in each group. **, $P \leq 0.05$ versus murine BSM strips overexpressing desmin in (A). **, $P \leq 0.05$ versus murine BSM strips overexpressing vimentin in (B). **, $P \leq 0.01$ versus murine BSM strips overexpressing desmin in (D). ǂǂ, $P \leq 0.01$ versus murine BSM strips overexpressing vimentin in (D).